Simulation of diblock copolymer surfactants. II. Micelle kinetics

Joshua A. Mysona, Alon V. McCormick, and David C. Morse

Phys. Rev. E **100**, 012603 — Published 8 July 2019

DOI: 10.1103/PhysRevE.100.012603

Simulation of Diblock Copolymer Surfactants. 2. Micelle Kinetics

Joshua A. Mysona, Alon V. McCormick, and David C. Morse*
Department of Chemical Engineering and Materials Science,
University of Minnesota, 421 Washington Ave. SE, Minneapolis, MN 55455, USA

Molecular dynamics (MD) simulations are used to measure dynamical properties of a simple bead-spring model of A-B diblock copolymer molecules, and to characterize rates and mechanisms of several dynamical processes. Dynamical properties are analyzed within the context of a kinetic population model that allows for both stepwise insertion and expulsion of individual free molecules and occasional fission and fusion of micelles. Kinetic coefficients for stepwise processes and micelle fission have been extracted from MD simulations of individual micelles. Insertion of a free surfactant molecule into a pre-existing micelle is shown to be a completely diffusion controlled process for the model studied here. Estimates are given for rates of rare events that create and destroy entire micelles by competing association/dissociation and fission/fusion mechanisms. Both mechanisms are shown to be relevant over the range of parameters studied here, with association/dissociation dominating in systems with more soluble surfactants and fission/fusion dominating in systems with less soluble surfactants.

I. INTRODUCTION

Surfactant solutions containing spherical micelles exhibit a variety of dynamical processes with widely varying time scales. The slowest processes in such systems are those that create or destroy entire micelles, and thereby change the total number of micelles in solution. Processes that change aggregation number of individual micelles without changing the number of micelles occur more frequently through expulsion and insertion of individual molecules. Internal relaxation processes that do not change aggregation number are faster still. Slow processes involving micelle creation and destruction play a crucial role in controlling the terminal rate of relaxation of dilute micellar solutions towards a new equilibrium state after a perturbation, and play an important role in the transport of copolymer to interfaces.

In this paper, we analyze rates of slow dynamical processes in a simple simulation model of a nonionic diblock copolymer surfactant. The model studied here is a bead-spring model of a highly asymmetric AB diblock copolymer with a minority B block dissolved in a matrix of A homopolymer. Equilibrium properties of the same model have been studied in a companion paper [1] (hereafter referred to as I). The work presented here combines the use of molecular dynamics (MD) simulations of individual micelles with analysis of a model of micelle population dynamics in which all parameters are determined from MD simulations. The primary goal of the study is to clarify the dominant mechanism of rare events that create and destroy entire micelles, which remains poorly understood despite decades of study and discussion. A secondary goal is to quantify the barriers associated with molecular exchange dynamics.

* Corresponding author, email: morse012@umn.edu

II. BACKGROUND

A. Experiments

Several experimental techniques have been used to study dynamics of micellar solutions in or near thermal equilibrium. Historically, the most important of these have been techniques that monitor relaxation of a micellar system to a new equilibrium state after the system is disturbed by small step change in temperature, pressure, or surfactant concentration [2–10]. Relaxation has been monitored in such experiments by measuring changes of conductivity in ionic systems, light scattering, and flourescence of probe molecules. Similar information about some systems has also been obtained from ultrasonic spectroscopy [6, 11–13].

Both relaxation and ultrasonic spectroscopy experiments have demonstrated the existence of two relaxation processes with disparate time scales, which are often referred to as the fast and slow processes. Corresponding relaxation times are denoted by τ_1 (the fast time) and τ_2 (the slow time). The fast process observed in relaxation experiments is believed to be a partial requilibration achieved by repartitioning of surfactant between micelles and free molecules after a disturbance, with negligible change in the number of micelles. The slow process is instead believed to be the result of a slower re-adjustment in the number of micelles [14–17].

A more recent generation of time-resolved neutron scattering (TR-SANS) experiments on non-ionic and block copolymer surfactants have made it possible to monitor the rate at which surfactants are exchanged between different micelles [18–20]. Exchange occurs primarily via random expulsion and insertion of individual molecules [19, 20]. The time scale over which the excess scattering signal measured in TR-SANS experiments decays is proportional to the time required for a majority of the surfactant molecules that are in a particular micelle at the beginning of the measurement to be replaced by molecules that were originally in other micelles. Be-

cause this exchange time is generally much less than the time required to create or destroy entire micelles, this technique is not sensitive to these slower processes.

The mechanisms of the fast relaxation process in relaxation experiments and of exchange in TR-SANS experiments are now reasonably well understood. The mechanism by which the number of micelles changes in the slow process of a relaxation experiment, however, remains controversial [17, 21–23]. The number of micelles in an equilibrated micellar solution could in principle change either by stepwise association and dissociation processes or by micelle fission and fusion. Stepwise association and dissociation are processes whereby an entire micelle can be created by association of free surfactant molecules or destroyed by dissociation into free molecules via random sequences of single-molecule insertion and expulsion events. Fission and fusion are processes in which the number of micelles can instead increase by one when a large micelle undergoes fission or decrease by one when two micelles undergo fusion. It has remained difficult for experiments that detect the existence of a slow process to conclusively rule out either mechanism.

B. Stepwise Kinetic Models

The simplest and most heavily studied theory of micelle dynamics is the stepwise model [14–17, 22, 24–29], which was originally developed by Aniansson and Wall [14–16]. This model assumes that fission and fusion rates are negligible, and that changes in the number of micelles thus occur only by stepwise association and dissociation. The resulting theory is closely analogous to the Becker-Döring theory of stepwise nucleation of a liquid from a supersaturated vapor [30], and so has also been referred to as the Becker-Döring theory [22].

The stepwise model predicts the existence of slow and fast processes with widely disparate time scales, as observed in experiments. The model predicts that the equilibrium rate of association events is proportional to the equilibrium concentration of very rare clusters of some critical aggregation number, which depends exponentially upon the free energy required to form such clusters. The stepwise model also makes non-trivial predictions regarding how the fast and slow times τ_1 and τ_2 depend on overall surfactant concentration. The rate τ_1^{-1} of the fast process is predicted to increase with increasing total surfactant concentration, and to vary approximately linearly with concentration at concentrations well above the critical micelle concentration (CMC). The rate τ_2^{-1} of the slow process is predicted to exhibit a non-monotonic dependence on concentration, with a maximum rate at a concentration slightly above the CMC, but to decrease with increasing concentration at concentrations well above the CMC [16, 17].

Predictions of the stepwise growth theory have been compared to observations of both the fast and slow relaxation times [16, 17]. Agreement between predictions and measurements of the fast relaxation time τ_1 is generally satisfactory, for experiments on both ionic and non-ionic surfactants[16, 31]. Agreement between predictions and measurements of the slow relaxation time τ_2, however, is often poor [16, 17, 22, 31]. A variety of experiments instead suggest that the slow process may occur in some systems primarily by fission and fusion, rather than by purely stepwise processes.

Experiments on ionic surfactant solutions in solutions of high ionic strength [16, 17] and on nonionic surfactants [17, 31, 32] have yielded rates for the slow process that increase monotonically with increasing surfactant concentration, in qualitative disagreement with predictions of the stepwise model. Experiments on ionic surfactants in systems with lower ionic strength instead exhibit a relaxation rate τ_2^{-1} that increases with copolymer concentration, in qualitative agreement with this model. Kahlweit and coworkers have argued on the basis of these observations that the slow process may occur primarily by fission and fusion in nonionic systems and in ionic systems at sufficiently high salt concentration, but by stepwise association and dissociation in ionic systems with sufficiently low ionic strength [17, 21], because fusion may be suppressed by electrostatic repulsions between micelles in ionic systems of low ionic strength.

Colegate and coworkers [22, 32] have compared measurements of τ_2^{-1} in micellar solutions of simple non-ionic surfactants to predictions of a stepwise model with physically realistic thermodynamic and kinetic parameters. The resulting model was found to predict values for τ_2^{-1} that are much less than those observed experimentally [22, 33], indicating the possibility of another mechanism.

Experiments on block copolymer surfactants in ionic liquid solvents have shown that the micelle hydrodynamic radius, as measured by light scattering, can change in response to signficant changes in temperature even in systems of essentially insoluble surfactants in which TR-SANS experiments show no evidence of exchange [34]. Since the absence of exchange indicates a low or even zero rate for all stepwise processes, this observation also suggests a role for fission and fusion.

C. Kinetic Models with Fission and Fusion

Several authors have constructed mathematical models of micelle kinetics that do allow for the possibility of fission and fusion of proper micelles, in addition to stepwise processes [29, 33, 35–37]. An early analysis of such a model was given by Dormidontova [35], who considered diblock copolymer micelles in a small molecule solvent. Dormidontova's analysis has been criticized for failing to enforce the principle of detailed balance [24]. Several authors have subsequently presented general equations for a model that allows for fission and fusion involving clusters of arbitrary size in a form that manifestly satisfies detailed balance [33, 36, 37].

At this point, the predictive power of population mod-

els that allow for fission and fusion is limited primarily by limited knowledge of values of rate constants for fission and fusion reactions. To estimate these rate constants, one must consider the magnitude of relevant kinetic barriers to fusion and/or fission. (Given knowledge of equilibrium free energies, an understanding of either fission or fusion would suffice because the two processes are related by detailed balance.) For block copolymer surfactants, a barrier to fusion can arise from repulsion between the polymeric coronas of different micelles. For ionic surfactants, a barrier to fusion instead arises primarily from electrostatic repulsion.

There has been little theoretical work on quantitative estimates of the barriers to micelle fusion or fission. A scaling theory of the barrier to fusion of block copolymer micelles has been presented by Halperin and Alexander [38]. The main limitations of this theory is that the scaling approach used there is appropriate only for very long, strongly insoluble copolymers, and does not yield reliable predictions for numerical prefactors in scaling relations for the barrier to fusion and other free energies.

In the absence of more reliable estimates of these barriers, several analyses of micelle kinetics that allow for fission and fusion have relied either on an assumption of diffusion limited fusion, or some *ad hoc* modification of this assumption [33, 35–37]. Assuming that fusion is diffusion limited is equivalent to assuming that the barrier to micelle fusion is negligible. This assumption thus overestimates the fusion rate, sometimes dramatically. It has been shown, however, that if fusion were diffusion limited, then fission and fusion reactions could easily dominate the overall rate of micelle creation and destruction, particularly in systems with a large barrier to the competing mechanism of stepwise association and dissociation (i.e., a large free energy of formation for critical clusters). Griffiths, Colegate and coworkers have compared experimental kinetic data for a nonionic alkyl - polyoxyethylene glycol surfacant to a kinetic model that employed a realistic model for the dependence of micelle free energy on aggregation number. To assess the effects of a barrier to fusion, these authors assumed that all fusion rate constants were lower than those obtained by assuming diffusion-limited fusion by a prefactor, which they treated as an adjustable parameter [22, 33]. They found that a purely stepwise model predicted unrealistically large values for τ_2, but that values of τ_2 comparable to those obtained in experiment could be obtained by assuming that fusion rates are 3-4 orders of magnitude slower than those predicted by a model of diffusion limited fusion.

D. Simulations

MD simulations of dynamical phenomena in micellar solutions have thus far been limited primarily to the study of either systems that are initially far from equilibrium or of relatively rapid relaxation processes in systems believed near equilibria (such as relaxation of chain conformation or counterion distribution). Simulations in which the initial state is a highly supersaturated solution of dissociated surfactants have been used to study the early stages of aggregation [39–41]. Simulations of the response of a pre-existing micelle to sudden changes in conditions (e.g., ionic strength) have shown that large changes can cause a micelle to undergo fission via a dumbbell shaped intermediate state [42–45]. Several simulations of dynamical properties near equilibrium have focused on processes involving single-molecule insertion and expulsion in model systems of relatively soluble surfactants [46, 47]. Pool and Bolhuis have also used an advanced sampling technique to study the free energy barriers to fission and fusion [48] in one model system, but did not compute absolute rates of fission and fusion or compare rates for different possible mechanisms of the slow process. There is a need for more systematic use of simulations to study rates and mechanisms of relatively slow dynamical processes in micellar systems and other self-assembled structures.

III. OVERVIEW

In the present work, we use MD simulations to estimate rate constants for elementary processes such as insertion, expulsion, and fission in a simple simulation model of block copolymer surfactants. The rate constants obtained from these simulations and the micelle free energies obtained in paper I are then used as input parameters to a population model that we use to compute overall rates of slow dynamical processes in an equilibrated solution. This combination of techniques allows us to estimate rates for some processes that would be too rare to be observed in brute force MD simulations of a micellar solution. The success of this procedure relies critically on the fact that the free energy required to form a micelle of arbitrary size has been accurately computed for the model of interest in paper I.

Rate constants for expulsion and insertion of single molecules are obtained from an analysis of simulations of systems that contain a single micelle in coexistence with a few free surfactant molecules. Knowledge of both micelle formation free energies and insertion and expulsion rate constants allows us compute rates of hypothetical stepwise micelle association and dissociation events.

Micelle fission is studied here by directly simulating spontaneous fission of pre-assembled micelles. These simulations of fission are performed on micelles that are somewhat larger the equilibrium size, for which fission is found to occur frequently enough to allow us to quantify rates. An upper bound on the maximum possible rate of spontaneous fission is also obtained by computing rates for a model in which fusion is assumed to be diffusion controlled. The resulting information about how fission rates depend on aggregation number then allows us to give meaningful estimates and bounds on overall

rates of fission in an equilibrated solution. We have not attempted to directly simulate fusion processes, but rely on the fact that rates for corresponding fission and fusion reactions must be equal in equilibrium, by the principle of detailed balance. A comparison of the resulting estimates of rates of fission/fusion to corresponding estimates of rates of stepwise association/dissociation allows us to shed light on the conditions under which one mechanism or the other dominates the overall rate of micelle birth and death.

The molecular dynamics (MD) simulations presented here all use a very simple bead-spring model of a highly asymmetric AB diblock copolymer surfactant in an A homopolymer solvent. This model is described in detail in I, and is merely summarized here for clarity. Each copolymer surfactant in this model is a chain of 32 beads with 4 B beads and 28 A beads. Each homopolymer solvent molecule is a chain of 32 A beads. We chose to use a polymeric solvent with the same number of beads as the copolymer because this allowed the use of very efficient semi-grand Monte Carlo techniques to measure equilibrium properties in paper I. Neighboring beads within a chain interact via a harmonic bond potential. All beads interact via a soft repulsive non-bonded pair potential of the type used in dissipative particle dynamics simulations. The interaction between a pair of particles of types i and j separated by a distance r is of the form $U_{ij}(r) = \epsilon_{ij}(1 - r/\sigma)^2/2$ for $r < \sigma$, with $U_{ij}(r) = 0$ for $r > \sigma$. Here, ϵ_{ij} is an interaction energy, which has a value $\epsilon_{AA} = \epsilon_{BB} = 25k_BT$ for interactions between beads of the same type, where k_B is Boltzmann's constant and T is absolute temperature. The repulsion between unlike A and B beads exceeds the repulsion between pairs of A beads or pairs of B beads by an amount controlled by a dimensionless parameter

$$\alpha = (\epsilon_{AB} - \epsilon_{AA})/k_BT \quad . \tag{1}$$

We have studied both equilibrium properties and dynamics at four values of $\alpha = 10$, 12, 14, 16.

All MD simulations presented here were peformed in the NPT ensemble using an integration algorithm based on that of Martyna, Tobias, and Klein [49]. All MD simulations were performed using an integration time step $\Delta = 0.005\tau_0$. Here, $\tau_0 = \sigma\sqrt{m_b/k_BT}$ denotes a Lennard-Jones time unit, in which m_b is a bead mass that is the same for all beads. We have compared results obtained with NPT simulations to results obtained from NVE molecular dynamics simulation performed with inital states generated from an NPT simulation, and confirmed that our use of a relatively weakly coupled thermostat and barostat used here did not effect any measured dynamical properties.

The remainder of this paper is organized as follows. Sec. IV presents the micelle population model used in the analysis of simulation data. Sec. V presents results for tracer diffusion coefficients for both free molecules and micelles, which are needed in analyses of other processes. Sec. VI presents an analysis of rate constants for insertion and expulsion of individual molecules from or into a micelle. Sec. VII also presents a similar analysis of rate constants for insertion and expulsion of copolmers into or out of a homopolymer droplet, which we compare to results obtained in Sec. VI in order to clarify the effect of the micelle corona on these processes. Sec. VIII is an analysis of the average micelle lifetime before dissociation occurs, which may be calculated from knowledge of the insertion and expulsion rate constants and the micelle free energies found in paper I. Sec. IX presents an analysis of how the intrinsic rate of spontaneous fission of a micelle depends on micelle aggregation number. Sec. X analyzes a model of that assumes diffusion limited fusion, which may also be used to calculate corresponding fission rates, and compares predictions of this model to those obtained from MD simulations.. Sec. XI calculates and compares the different methods of estimating the average time for a randomly selected micelle to undergo spontaneous fission, which we refer to as the equilibrium fission lifetime. Conclusions are discussed in XII.

IV. POPULATION MODEL

All simulations presented in this paper are interpreted within the context of a simple population model for a dilute micellar solution containing aggregates of different sizes. Let n or n' denote the number of copolymer surfactant molecules in a particular species of aggregate, where $n = 1$ denotes free molecule. Let c_n denote the number concentration of aggregates that contain n molecules, or "n-mers", while c_1 is the concentration of free surfactant molecules, or "unimers". The equilibrium concentration of n-mers is denoted by c_n^*, and has been computed for the simulation model of interest in paper I.

We consider a population model that allows for both stepwise reactions (i.e., insertion of a unimer into a micelle or expulsion of a unimer from a micelle) and less frequent reactions involving fission and fusion of larger aggregates [33, 36, 37]. Let $r^+_{n,n'}$ denote the rate of fusion of clusters of aggregation number n and n', per unit volume and per unit time. Let $r^-_{n,n'}$ denote the corresponding rate of the fission reaction in which clusters of aggregation number $n+n'$ fission into daughters of specified aggregation number n and n'. We assume that fusion is a second order reaction, controlled by the rate law

$$r^+_{n,n'} = k^+_{n,n'} c_n c_{n'} \quad , \tag{2}$$

and that fission is controlled by a first-order rate law

$$r^-_{n,n'} = k^-_{n,n'} c_{n+n'} \quad , \tag{3}$$

where $k^+_{n,n'}$ and $k^-_{n,n'}$ are rate constants for these elementary processes. The insertion reaction, in which a free surfactant molecule is inserted into a micelle of size n to create a micelle of size $n + 1$ is a special case of the fusion reaction in which $n' = 1$. The corresponding expulsion reaction is a special case of fission with $n' = 1$.

The time dependence of m-mer concentration $c_n(t)$ is controlled for all $m \geq 1$ by a master equation

$$\frac{dc_n(t)}{dt} = \sum_{n'=1}^{n/2} J_{n-n',n'} - \sum_{n'=1}^{\infty} \nu_{n,n'} J_{n,n'} \quad . \tag{4}$$

Here, $J_{m,m'}$ is a flux given by the difference

$$J_{n,n'} = r^+_{n,n'} - r^-_{n,n'} \tag{5}$$

between the rate of fusion of clusters of sizes n, n' and the rate of fission of clusters of size $n + n'$ into reaction products of these sizes. The quantity $\nu_{n,n'}$ is a stoichiometry coefficient equal to the number of aggregates of size n (or n') consumed per fusion of clusters of size n and n', which is given by $\nu_{n,n'} = 1$ for all $n \neq n'$ but $\nu_{n,n'} = 2$ in the special case $n = n'$.

The first summation in Eq. (4) represents the net rate of production of n-mers produced by fusion of smaller aggregates of size m' and $n - n'$, minus the rate of fission of n-mers into smaller aggregates. To avoid double counting of equivalent reactions, the sum over m' in this sum is constrained to values for which $n' \leq n - n'$. This constraint yields an upper bound of $m' = m/2$ for even n and $n' = (n - 1)/2$ for odd n. The second sum in Eq. (4) is the net rate of production of n-mers via fission of larger aggregates into daughters in which at least one of the fission products is an n-mer, minus the rate of fusion of n-mers with clusters of any other size.

For the special case of unimers, or $m = 1$, the first term in Eq. (4) is absent, giving a rate of change

$$\frac{dc_1(t)}{dt} = -\sum_{n'=1}^{\infty} J_{n',1} = \sum_{n'=1}^{\infty} (r^-_{n',1} - r^+_{n',1}) \quad . \tag{6}$$

This is simply the difference between the overall rates of stepwise expulsion and stepwise insertion.

The principle of detailed balance requires that, in equilibrium,

$$r^+_{n,n'} = r^-_{n,n'} \tag{7}$$

for all $n, n' \geq 1$ or, equivalently, that $J_{n,n'} = 0$. Combining this with the fission and fusion rate laws, Eqs. (2) and (3), yields the more explicit requirement that

$$k^+_{n,n'} c^*_n c^*_{n'} = k^-_{n,n'} c^*_{n+n'} \quad , \tag{8}$$

for all $n, n' \geq 1$. Because this condition relates fission and fusion rate constants, knowledge of either fission or fusion rate constants for all pairs of aggregation numbers and of c^*_n for all n is thus sufficient to specify all parameters in the kinetic model.

A. Stepwise (Becker-Döring) Model

The stepwise or Becker-Döring model assumes that the only relevant reactions are stepwise insertion and expulsion reactions. The master equation for this restricted model can be obtained by assuming that the only non-negligible terms in Eq. (4) are those with $n' = 1$. In discussions of the step-wise model, we hereafter adopt the simplified notation

$$J_n \equiv J_{n,1} \quad , \quad k^\pm_n \equiv k^\pm_{n,1} \tag{9}$$

to refer to fluxes and rate constants for stepwise processes. In this notation

$$J_n = k^+_n c_n c_1 - k^-_n c_{n+1} \quad , \tag{10}$$

is the net rate at which clusters of size n are transformed into clusters of size $n + 1$ via insertion of unimers into n-mers and expulsion of unimers from $(n + 1)$-mers.

The time evolution of the stepwise model is controlled by

$$\frac{dc_n(t)}{dt} = J_{n-1} - J_n \tag{11}$$

for all $n > 1$, and

$$\frac{dc_1(t)}{dt} = -\sum_{n=1}^{\infty} J_n \tag{12}$$

for $m = 1$ (i.e., unimers).

The detailed balance for the stepwise model requires that

$$\frac{k^+_n c_1}{k^-_n} = \frac{c^*_{n+1}}{c^*_n} = e^{-\Delta W_n / k_B T} \quad , \tag{13}$$

in which $\Delta W_n \equiv W_{n+1} - W_n$. Using this relation, J_n may also be expressed as a difference

$$J_n = -k^-_n \left(c_{n+1} - e^{-\Delta W_n / k_B T} c_n \right) \quad , \tag{14}$$

with no explicit dependence on k^+_n.

If $\Delta W_n \ll k_B T$ for all n of interest, then we may approximate Eq. (11) by a diffusion equation in which n is treated as a continuous variable. In this limit, we obtain

$$\frac{\partial c_n}{\partial t} = \frac{\partial}{\partial n} \left(k^-_n \left(\frac{\partial c_n}{\partial n} + c_n \frac{\partial}{\partial n} \left(\frac{W_n}{k_B T} \right) \right) \right) \quad . \tag{15}$$

This is a Fokker-Planck equation for the evolution of $c_n(t)$ due to diffusion of aggregation number n under the influence of a potential W_n, with an effective diffusivity given by the expulsion rate constant k^-_n.

B. Diffusion Controlled (Smoluchowski) Model

The range of possible values for fusion rate constants is limited by the rate at which aggregates randomly collide via diffusion. The classical Smoluchowski model of fast binary reactions among hypothetical spherical particles assumes that any two particles that diffuse close enough

to touch will react, and thus assumes that rates are completely diffusion controlled. In the Smoluchowski model, the rate constant $k^+_{n,n'}$ is given by an expression of the form

$$k^+_{n,n'} = \nu^{-1}_{m,m'} 4\pi R_{n,n'}(D_n + D_{n'}) \tag{16}$$

in which D_n is the tracer diffusion coefficient for an n-mer, and $R_{n,n'}$ is an effective capture radius for collision of aggregates of size n and n'. In the classical Smoluchowski model of interacting spherical particles this binary capture radius is assumed to be equal to the sum

$$R_{n,n'} = R_n + R_{n'} \tag{17}$$

of the hard-sphere radii of the two particles.

The stoichiometric factor of $\nu^{-1}_{n,n'}$ in Eq. (16) is equal to 1 for all $n \neq n'$ and equal to 1/2 in the special case $n = n'$. Note that this factor cancels the factor of $\nu_{n,n'}$ in the term representing consumption of n-mers in the master equation, Eq. (4). The overall rate of consumption per unit volume of n-mers by fusion with n'-mers is thus given by $4\pi R_{n,n}(D_n + D_{n'})c_n c_{n'}$ for all n', with no stoichimetric prefactor. The corresponding probability per unit time that a randomly chosen labelled n-mer will be anhihilated by colliding with any n'-mer is given for any n' by $4\pi R_{n,n'}(D_n + D_{n'})c_{n'}$. This predicted rate of collision between a labelled n-mer and any n'-mer can be obtained by considering diffusion of a surrounding concentration $c_{n'}$ of n'-mers to an absorbing spherical boundary of radius $R_{n,n'}$ surrounding a labelled n-mer.

In this work, we consider a version of the Smoluchowski model in which we approximate the core regions of AB block copolymer micelles as spherical particles that fuse upon contact, and thus take the radii R_n and $R_{n'}$ in Eq. (17) to be equal to the micelle core radii. Because fusion and fission rates are related by the principle of detailed balance, a prediction for the fusion rate $k^+_{n,n'}$ can be combined with knowledge of the equilibrium concentrations to predict corresponding rate constants for fission. The assumption of diffusion limited fusion can thus be used as the basis of a complete but very approximate theory of fission and fusion rates.

We do not expect the assumption of diffusion-controlled fusion to accurately describe most real systems. Either the repulsion between micelle coronas in nonionic block copolymer systems or the electrostatic repulsion between micelles in ionic systems can presumably create a signficant barrier to fusion. Predictions of the diffusion-controlled model are nonetheless considered here because the model has used as the starting point of several previous analyses, and because it provides a useful upper bound on the range of possible values for fusion rate constants.

V. DIFFUSION

Values of the tracer diffusion coefficients for unimers and for micelles of all sizes are needed in order to predict diffusion-controlled limits for rates of insertion and fusion. The tracer diffusion coefficient D for either a unimer or a micelle can be obtained from a measurement of mean-squared displacement as a function of time. At long times, the mean-squared displacement (MSD) $\langle(\Delta R)^2\rangle$ of the center-of-mass of a molecule or cluster in a large simulation cell varies with time t as

$$\langle(\Delta R)^2\rangle = 6Dt \tag{18}$$

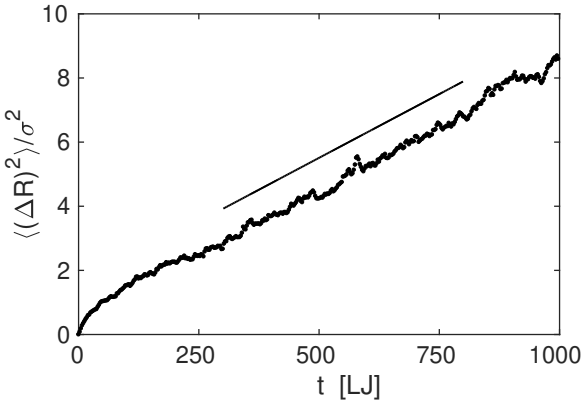

FIG. 1. Mean squared displacement $\langle(\Delta R)^2\rangle$ of a micelle center of mass as a function of time t for a micelle of aggregation number $m = 60$ and $\alpha = 16$ in a box 40σ on a side. The solid line shows the slope of a linear fit to the late time behavior, and has been displaced above the data for visibility. After correcting for finite size effects, we obtain a diffusivity of $D = 0.001926\sigma^2/\tau_0$ for this micelle, where σ is the range of the DPD potential and τ_0 is the Lennard-Jones time unit.

A typical mean squared displacement curve for a micelle is shown in Figure 1. We have determined apparent diffusivities for both individual copolymers and micelles of varying sizes by fitting a line to data for $\langle(\Delta R)^2\rangle$ vs. t at long times. Results for micelle MSD were obtained for each choice of parameters considered here from an average of 144 independent simulations of systems that each contain a single micelle simulation over a duration of 10^4 LJ time units in a cubic simulation boxes of size $L = 25.2\sigma$ or larger.

When this analysis of MSD was applied to simulations that contain one micelle in a simulation cell that is only a few times larger than the micelle, the resulting apparent values for D were found to depend noticeably on the size of the periodic simulation cell [50, 51]. This finite-size effect in simulations of a single micelle is a well understood result of the hydrodynamic interaction of each micelle with its periodic images [50, 52]. Values for the diffusion coefficient reported here were thus corrected to account for this hydrodynamic effect in order obtain the diffusion coefficient that would be obtained in a macroscopic system, which we denote by D. The required correction is discussed in Appendix A.

We first consider tracer diffusion of individual diblock copolymers in a hompolymer melt. We obtain a tracer

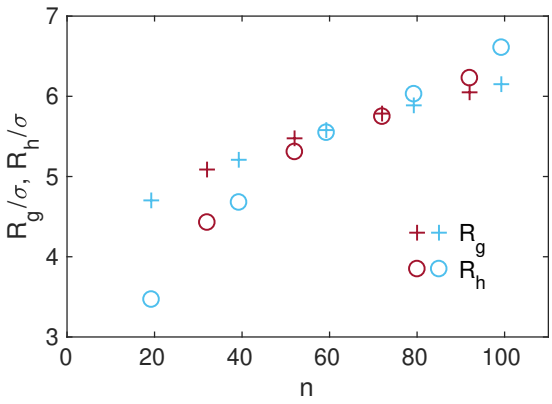

FIG. 2. The radius of gyration R_g (+ symbols) and hydrodynamic radius R_h (open circles) plotted vs. aggregation number n. Different colors represent results obtained with $\alpha = 16$ (light blue) and $\alpha = 12$ (dark red).

diffusivity of $D = 0.0125\ \sigma^2/\tau_0$ for A homopolymers, corresponding to copolymers with $\alpha = 0.0$, and $D = 0.0117\ \sigma^2/\tau_0$ for copolymers with $\alpha = 16$, the highest value of α considered here. Because this diffusivity was found to depend only weakly on α, we used the homopolymer ($\alpha = 0$) tracer diffusivity as an approximation for the copolymer diffusivity in subsequent analysis.

Results for the diffusion coefficient D for a micelle can be used to define a corresponding micelle hydrodynamic radius R_h by using Stokes-Einstein formula

$$D = k_B T/(6\pi\eta_0 R_h) \quad , \tag{19}$$

where η_0 is the zero shear viscosity of the surrounding solvent, which in this case is a homopolymer liquid.

Colleague T. Ghasimakbari has measured the stress relaxation modulus $G(t)$ and zero shear viscosity $\eta_0 = \int_0^\infty G(t)dt$ of a homopolymer melt simulated with the model used here. He found that the dependence of these quantities on time and chain length is very well described by a Rouse model [53] with a viscosity $\eta_0 = 7.92\ k_B T\tau_0/\sigma^2$ for chains of 32 beads.

Figure 2 shows simulation results for the dependence of both radius of gyration R_g (+ symbols) and hydrodynamic radius R_h (circles) upon n, using data obtained from two different values of $\alpha = 12$ and $\alpha = 16$. Results obtained with different values of α nearly collapse when plotted vs. n, indicating that results for R_h and R_g at any specified value of n are almost independent of α. Results for R_h shown in this figure were obtained from estimates of diffusivity in an infinite domain, after correcting for hydrodynamic finite size effects. The hydrodynamic radius R_h is found to vary somewhat more strongly with n than the radius of gyration R_g, but always remains comparable to R_g.

VI. INSERTION AND EXPULSION

This section presents an analysis of rate constants for insertion of a free surfactant molecule into a micelle and for expulsion of a single surfactant molecule from a micelle. Throughout this section, we use the symbols $k_n^+ = k_{n,1}^+$ and $k_n^- = k_{n,1}^+$ for insertion and expulsion rate constants, respectively.

A. Methodology

Insertion and expulsion rate constants have been inferred from simulations of sytems that each contain a single micelle in coexistence with a few free surfactant molecules within a periodic cubic unit cell. In a system with exactly one micelle of size n, we expect free molecules to be expelled from the micelle at a rate k_m^- and inserted at a rate $k_m^+ c_1$, where c_1 is the concentration of free molecules in coexistence with the micelle. Once the simulation has reached equilibrium over long times the average of these two rates must be equal.

We define the observed rate of insertion and expulsion in such a simulation as follows: At each instant, we identify a set of copolymer molecules that are "inside" the micelle, and another set that are far "outside". Which copolymer molecules are inside the micelle is determined by a cluster analysis that identifies molecules for which the atoms of the core-forming B block are in close contact. (This algorithm is discussed in greater detail in paper I.) A copolymer is defined to be "outside" if the distance from the center of mass of the micelle to the B bead at the A-B junction (the B bead that is bonded to an A bead) exceeds some cutoff distance R_o, which we refer to as the outer radius. We assign every molecule a variable with possible values "in" or "out" indicating whether that molecule was most recently inside or outside, in the sense described above. The value of this variable changes from in to out only when a molecule that was most recently inside the micelle diffuses far enough from the micelle be relabelled as "out". Similarly, the label is changed from out to in whenever a micelle that was most recently "outside" is incorporated into the micelle. If a molecule leaves the micelle and is then reincorporated back into the micelle before reaching a distance R_o from center of the micelle, it is thus treated as if it never left the micelle.

The observed insertion rate, denoted by F, is given by the rate (number per time) at which surfactant molecules that are labelled "out" enter the micelle. Similarly, the observed explusion rate is given by rate at which molecules that have been expelled from the micelle but are labelled "in" diffuse far enough from the center of the micelle to be relabelled as "out". On average, in equilibrium, these insertion and expulsion rates must exactly balance. The value of the insertion rate $F(R_o)$ obtained by this method depends somewhat on the choice of the outer radius R_o, but approaches a limiting value in the

limit $R_o \to \infty$, denoted by

$$F_\infty \equiv \lim_{R_o \to \infty} F(R_o) \quad . \tag{20}$$

We estimate the limiting value F_∞ by an extrapolation procedure that is described below.

The limiting value F_∞ represents the rate at which expelled molecules irreversibly escape a micelle, or at which the micelle capture molecules that originate from distant points within a solution (e.g., from other micelles within a dilute micellar solution). The value for the macroscopic insertion rate constant k_n^+ for a micelle of aggregation number n in a dilute micellar solution is thus taken to be related to F_∞ by the relations

$$F_\infty = k_n^+ c_1 \quad , \tag{21}$$

where c_1 is the average concentration of free molecules under the conditions used in the simulation. Because the instantaneous aggregation number of the micelle in such a simulation fluctuates slightly as molecules are inserted and expelled, an estimate of k_n^+ is obtained from a simulation in which the average aggregation number of the micelle (excluding free molecules) is equal to n. This measurement is repeated for systems with different numbers of copolymer molecules and different values of α.

B. Dependence of Flux on Outer Radius

Our extrapolation of results obtained with a finite outer radius R_o to the limit $R_o \to \infty$ is based on a simple diffusion model of the dependence of the insertion rate F on on R_o. In this model, we treat chain insertion as diffusion to a micelle with an absorbing boundary with some effective capture radius R_c. We treat molecules that are labelled "in" and "out" as two different species that are interconverted by reactions that occur at the inner and outer boundary of a spherical annulus. Molecules that are labelled "out" are created (i.e., relabelled) at a steady rate F along the surface of a sphere of radius R_o around the center of the micelle, and are destroyed (or absorbed by the micelle) along a surface of radius R_c, the effective capture radius. Let $c(r)$ denote the concentration of copolymer molecules that are labelled "out" at points a distance r from the center of a micelle. Because all molecules that lie a distance greater than R_o from the micelle are labelled "out", the concentration of such molecules must equal the total free molecule concentration c_1 for all $r \geq R_o$. To compute $c(r)$, we thus solve a steady-state diffusion equation $0 = \nabla^2 c$ in the region $R_c < r < R_o$ subject to a boundary condition requiring that $c(R_o) = c_1$ along the outer boundary $r = R_o$ and an absorbing boundary condition requiring that $c(R_c) = 0$ at the effective capture radius $r = R_c$. The solution to this diffusion problem yields a concentration that depends on radius r as

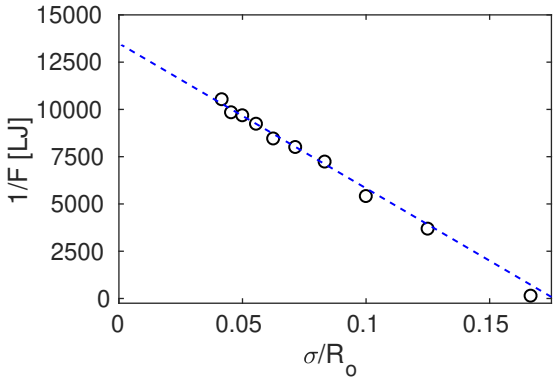

FIG. 3. Inverse insertion flux $1/F$ vs. inverse outer radius $1/R_o$, computed using data for single micelle of average aggregation number $n = 80$ at $\alpha = 12$ at several values of R_o. Inverse flux is measured in inverse Lennard-Jones time units.

$$c(r) = c_1 \frac{R_c^{-1} - r^{-1}}{R_c^{-1} - R_o^{-1}} \quad . \tag{22}$$

The corresponding flux of labelled molecules into the micelle satisfies the equation

$$\frac{1}{F} = \frac{1}{F_\infty} - \frac{1}{4\pi D c_1 R_o} \tag{23}$$

where D is the copolymer diffusivity, and where

$$F_\infty = 4\pi D R_c c_1 \tag{24}$$

is the limiting value of the flux in the limit $R_o \to \infty$.

The validity of Eq. (23) can be tested by plotting values of the inverse flux $1/F$ obtained using different values of R_o as a function of $1/R_o$. Because the copolymer diffusivity D and free copolymer concentration c_1 have been measured independently, the only free parameter in Eq. (24) is the extrapolated flux F_∞. Figure 3 shows an example of such a plot. The results shown here for different values of R_o were computed by simply postprocessing the same set of MD trajectories using different values R_o. The line in this plot was constructed using the predicted slope $1/(4\pi D c_1)$, computed using independenty measured values of D and c_1. The intercept of $1/F_\infty$ was chosen to fit this data. The quality of the fit confirms the validity of the proposed model for the dependence on R_o, and provides a straightforward method to determine F_∞ for each simulation.

C. Discussion

The above analysis of values of F_∞ was performed for micelles of varying aggregation number n for each of the four values of α considered here. The value of F_∞ obtained from each simulation was then used to compute

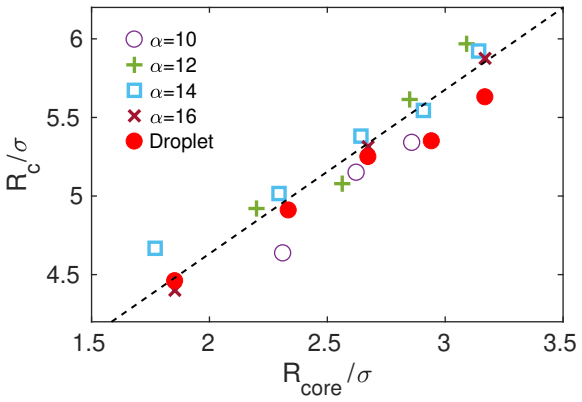

FIG. 4. Effective capture radius R_c for micelles and homopolymer droplets of differing aggregation number n plotted vs. the micelle core radius R_{core}. Data for micelles is shown for $\alpha = 10$, 12, 14, and 16 on a single graph, with distances in units in $\sigma = 1$. Corresponding results obtained from insertion and expulsion of copolymers into a homopolymer droplet at $\alpha = 12$ are show as solid red circles. The dashed line is the best global fit line drawn through the data, given by $R_c = 1.04R_{\rm core} + 2.55$.

a corresponding value of the effective capture radius R_c, by applying Eq. (24). Figure 4 shows a compilation of results for R_c plotted vs. the nominal micelle core radius $R_{\rm core}$. The nominal core radius $R_{\rm core}$ shown here is computed for a micelle of aggregation n by assuming a spherical micelle core and equating the core volume $4\pi R_{\rm core}^3/3$ to the expected volume $N_B n v$ of the monomers in the core block of n molecules, where $N_B = 4$ is the number of beads in each core-forming B block and $v = 1/c$ is the average volume per bead in the system of interest, for which we use $c = 3.0\sigma^{-3}$. Very similar values of R_c are obtained for systems with the same values of n and $R_{\rm core}$ but different values of α, as shown by the near collapse of data from different values of α in Figure 4. The dependence of the capture radius R_c on the core radius $R_{\rm core}$ is reasonably well described by a simple linear function

$$R_c(M) = R_{\rm core}(M) + \Delta \quad , \tag{25}$$

which is shown by the dashed line in Figure 4, in which Δ is a distance $\Delta = 2.55\sigma$.

Eq. (25) can be motivated by a simple picture of insertion as a diffusion-limited reaction between a spherical micelle core of radius $R_{\rm core}$ and a copolymer that acts as a sphere of effective radius Δ. If insertion were diffusion controlled but copolymer surfactants were point-like objects that are captured whenever they touch the micelle core, we would expect a capture radius $R_c = R_{\rm core}$. The fact that the effective capture radius is actually larger than the core radius is presumably a result of the fact that the copolymer is not a point particle, but is instead an extended object. Because of the strong effective attraction between B monomers in an A matrix, we assume that a copolymer diffusing near a micelle is nearly certain to be captured as soon as any monomer in the B block of the micelle comes in contact with the core of the micelle. Because the copolymer is an extended object, this first contact may occur when the center of hydrodynamic resistance of the molecule and the junction between the A and B blocks both remain outside the core, giving an effective capture radius somewhat larger than the core radius.

The above discussion is based on an assumption that insertion is diffusion controlled. Consider instead what we would expect to see if the micelle corona created a large barrier to insertion. In this case, the existence of a barrier would yield an insertion rate F much less than predicted by a diffusion-controlled model. Because R_c is proportional to F, by Eq. (24), existence of a signficant barrier to insertion would thus yield an effective capture radius signficantly *less* than the actual core radius. Observation of an effective capture radius slightly greater than the core radius thus implies that the corona does not create a signficant barrier to insertion, and that insertion must thus be at least approximately diffusion controlled.

VII. INSERTION INTO A DROPLET

The above analysis of effective capture radii for micelles suggests that, in the model studied here, insertion is at least approximately diffusion controlled. To make this statement more precise, we need to introduce an appropriate definition of what we would mean to say that this process was completely diffusion controlled. We are primarily concerned here with the possible effects of the corona of the micelle, which can produce a barrier to insertion. To define what we mean by diffusion controlled, or barrierless, insertion, we have thus chosen to compare our results for insertion of a copolymer molecule into a copolymer micelle to results for insertion of a copoymer into a liquid droplet of B homopolymers, and compare results for a micelle and liquid droplet containing an equal number of B monomers. Such a droplet acts as a model of the core of a micelle with no corona.

To create a homopolymer droplet, we simply create a system containing $N = 20 - 100$ short B homopolymer chains within a matrix of A homopolymers. Each of the B chains contains 4 B beads (which is the length of core block of our copolymers), while each A homopolymer contains 32 beads. The repulsion between A and B causes the homopolymer to form a liquid droplet with a structure similar to that of the micelle core. To measure the effective radius for capture of a copolymer by such a droplet we then add a few AB copolymers (much fewer than the number of B homopolymers) to the same system, measure rates of insertion of copolymers into a droplet using the method described above for a micelle, and convert the results into an estimated capture radius R_c

Resulting values for the capture radius R_c of a liquid

droplet are plotted vs. $R_{\rm core}$ in Figure 4 as solid circles, alongside corresponding results for the capture radii of micelles. The core radius $R_{\rm core}$ for a droplet is computed using a procedure analogous to that used for micelles, by setting the volume of a sphere of radius $R_{\rm core}$ equal to the volume nN_Bv computed using the average number n of homopolymers in the core, excluding any that escape into solution. When plotted vs. $R_{\rm core}$, results for the effective capture radii of homopolymer droplets all lie within the the narrow band of values obtained for capture radii of micelles. The fact that we obtain nearly identical results for R_c for a droplet and a micelle of equal core radius demonstrates that the corona does not cause any measurable barrier to insertion. In the model studied here, insertion is thus completely diffusion controlled.

VIII. EQUILIBRUM DISSOCIATION LIFETIME

In this section, we compute the average rate at which micelles would be created and destroyed by association and dissociation, in the absence of fission and fusion. Because we neglect the possibility of fission and fusion, the analysis is based on a completely stepwise model. As a measure of the frequency of dissociation events, let τ_d denote the average time before a randomly selected micelle in equilibrated solution would undergo stepwise dissocation, in the absence of fission and fusion. We refer to τ_d as the equilibrium dissociation lifetime. The value of τ_d depends on the overall copolymer concentration. All values reported here are computed for systems at a concentration twice the critical micelle concentration.

To define and compute τ_d, we consider the predictions of the stepwise kinetic model for the following thought experiment: Imagine that at some time $t = 0$, we identify and somehow label all proper micelles of aggregation number greater than some cutoff size. Imagine that we then keep track of fluctuations in the aggregation number of each micelle in this labelled population, and note when each of them undergoes complete dissociation into unimers. Let $P(t)$ denote the probability that a micelle that had an aggregation number $n > b$ at $t = 0$ has survived to time t without undergoing dissociation. Because dissociation is a rare, random event, we expect $P(t)$ to decay exponentially at long times, giving $P(t) \propto e^{-t/\tau_d}$, where τ_d is the desired dissociation lifetime.

The computation of τ_d is discussed in detail in appendix B and summarized more briefly here. The micelle lifetime can be computed using a slight modification of the method normally used to compute rates of stepwise nucleation in the Becker-Döring model. In this approach, one considers a pseudo-steady-state solution to the stepwise kinetics model in which the distribution $c_n(t)$ of surviving micelles closely resembles the equilibrium distribution c_n^* at values of n near the most probably value $n_{\rm e}$, but in which there is a small nonzero flux J_n from the micellar region to the submicellar region. This flux J_n is assumed to be nearly independent of n over a range of values of n near the transition state value $n_{\rm t}$. The resulting analysis is simply a discrete version of Kramer's method treating diffusion over a barrier. Similar answers's can be obtained by applying Kramer's analysis to the continuum diffusion equation given in Eq. (15).

When applied to the present problem, the Becker-Döring analysis yields a lifetime

$$\tau_d = Q \sum_{n=1}^{n_{\rm e}} \frac{1}{k_n^-} e^{W_{n+1}/k_BT} \quad , \tag{26}$$

in which

$$Q = \sum_{n=n_{\rm t}}^{\infty} e^{-W_n/k_BT} \tag{27}$$

is a partition function for a polydisperse micelle.

An analytic approximation for τ_d can be obtained by approximating the summands in Eqs. (26) and (27) by Gaussians and the sums by integrals. This yields a rate

$$\tau_d^{-1} \simeq \frac{k_{n_{\rm t}}^+}{2\pi\sigma_e\sigma_t} c_1 e^{-\Delta W_d/k_BT} \quad , \tag{28}$$

in which

$$\Delta W_d = W_{n_{\rm t}} - W_{n_{\rm e}} \tag{29}$$

is the barrier to dissociation. Here, σ_e is the standard deviation of n about $n_{\rm e}$ in the Gaussian approximation for e^{-W_n/k_BT} in Eq. (27), while σ_t is the standard deviation in the Gaussian approximation for e^{+W_n/k_BT} in Eq. (26). In Eq. (28), we have chosen to use the detailed balance condition to express the expulsion rate constant $k_{n_{\rm t}}^-$ by a product $k_{n_{\rm t}}^+ c_1$.

The factors of c_1 and $e^{-\Delta W_d/k_BT}$ in Eq. (28) both decrease rapidly with increasing α or, more generally, decreasing surfactant solubility. Other quantities in this equation, including the insertion rate $k_{n_{\rm t}}^+$, are much less sensitive to changes in surfactant solubility. All results reported here are for situations where $c_1 = c_c$. Values of c_c for this model decrease by approximately a factor of 23 between $\alpha = 10$ and $\alpha = 16$. Values of ΔW_d obtained in paper I range from only $3k_BT$ at $\alpha = 10$ to $14k_BT$ at $\alpha = 16$, corresponding to a change in $e^{-\Delta W_d/k_BT}$ by a factor of approximately 0.7×10^5. The most important factor controlling the decrease in the rate of dissociation with increasing α is thus the decrease in the Boltzmann factor associated with the free energy barrier ΔW_n, though the decrease in the unimer concentration also contributes.

Numerical results for the dependence of τ_d on α are shown in Fig. 5. The lifetime τ_d increases by approximately a factor of 10^6 as α increases from 10 to 16. As noted above, most of this increase is a result of an increase with increasing α in the free energy ΔW_d required to shrink an equilibrium micelle to the critical aggregation number $n_{\rm t}$ by expelling unimers. The value of $\tau_d \simeq 10^{13}\tau_0$ obtained at $\alpha = 16$ corresponds to approximately 10^{15} MD steps. Stepwise dissociation events

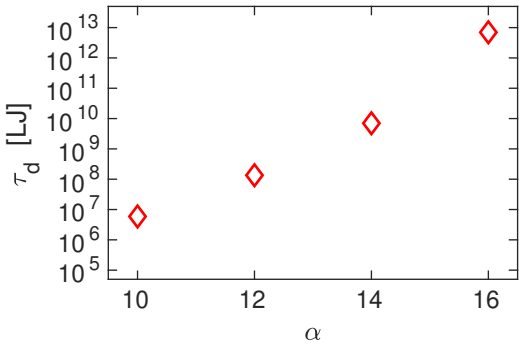

FIG. 5. Calculated equilibrium dissociation lifetime τ_d plotted against α. This lifetime increases by approximately 10^6 over the range $\alpha = 10 - 16$.

would thus be far too infrequent to be observed in brute force MD simulation, but can be accurately modelled by the combination of techniques used here.

It is worth noting that the dissociation lifetime τ_d considered here is not exactly equivalent to the "slow" relaxation time τ_2 predicted by the stepwise model to describe relaxation after a small perturbation. The dissociation lifetime τ_d is the average time it would take a randomly chosen micelle in an equilibrated solution to be destroyed by stepwise dissociation, in the absence of fission or fusion. The slow relaxation time τ_2 is instead the time required for a micellar solution to reach a new equilibrium state with a new micelle number concentration after equilibrium is disturbed by a step change in, e.g., temperature or total surfactant concentration. In appendix B, we compute τ_d by computing the rate at which a subpopulation of micelles that were present at some time $t = 0$ undergo dissociation. Because the solution remains in equilibrium, the unimer concentration c_1 is assumed to remain constant during this process. In the calculation of τ_2 by the stepwise model, as first given by Aniansson and Wall [14–16], one must instead allow for the fact that c_1 and average micelle aggregation number both change during the slow relaxation process. Both τ_d and τ_2 are proportional to an Arrhenius factor of e^{-W_d/k_BT}, and thus both become very large in systems with $W_d \gg k_BT$. The slow time τ_2 is, however, always less than τ_d, as a result of changes in c_1 during relaxation that tend to accelerate approach to a new equilibrium state.

IX. INTRINSIC FISSION RATES

We now focus on quantifying rates of spontaneous fission. The total rate of fission of micelles of a specified aggregation number n (n-mers) into daughters of all possible sizes can be expressed as product $k_n^{fis}c_n$, in which k_n^{fis} is a quantity that we will call the intrinisc rate constant for n-mers. This quantity is simply given by the sum

$$k_n^{fis} = \sum_{n'=1}^{n/2} k^-_{n',n-n} \tag{30}$$

of the rate constants for fission of n-mers into daughters of all possible pairs of sizes. We define a corresponding time scale τ_n^{fis} that is given by the inverse

$$\tau_n^{fis} \equiv 1/k_n^{fis} \quad , \tag{31}$$

and refer to τ_n^{fis} as the intrinsic fission lifetime for n-mers.

In this section, we present the results of MD simulations in which we have determined τ_n^{fis} for micelles of varying aggregation number n by directly observing spontaneous fission of artificially assembled metastable micelles. The lifetime τ_n^{fis} is found to decrease rapidly with increasing n. For micelles with n similar to the most probable value n_e, this lifetime is found to be too long to allow direct observation of fission in long MD simulations. The simulations presented are instead performed using larger, less stable micelles in order to obtain computationally accessible fission lifetimes.

A. Methodology

For each value of α, we have performed fission simulations at several values of N, the total number of molecules in the simulation cell. For each choice of α and N, we created an ensemble of n equivalent systems, each of which initially contains a single preassambled micelle containing all N copolymers. All the systems in each such ensemble are then simulated for an equal time T that is chosen to be long enough to observe spontaneous fission of the micelle in a significant fraction of the systems. All of the results presented here were obtained using ensembles of $n = 20$ such equivalent systems.

The pre-assembled micelle in each such system was created by first generating an initial configuration in which copolymers are distributed randomly throughout the simulation unit cell, and then running a short preparatory MD simulation with an artificial external potential that strongly attracts B monomers (those in the copolymer core block) to a spherical region of radius comparable to the expected radius of the micelle core. The external potential was then turned off to begin the dynamical simulation, during which the micelle can undergo fission.

The time required for the NPT integrator to reestablish the target temperature and pressure after turning off the external potential was small compared to the time required for any other equilibration process (i.e., the time for the radius of gyration to equilibrate), and much smaller than the average fission time. After this, the micelle undergoes a period of local structural equilibration, during which the micelle shape begins to fluctuate. Over a somewhat longer period, the micelle also generally expels a few molecules, creating a metastable local

equilibrium state in which the micelle is in equilibrium with a few free copolymers.

Figure 6 shows an example of the time dependence of the radius of gyration of the micelle core (i.e., of the collection of B monomers of molecules in the micellar cluster) and of the number of free molecules (molecule outside the cluster) as a function of time t, for $\alpha = 14$. In this example, the radius of gyration of the cluster has equilibrated after roughly 10^3 LJ time units (i.e., approximately 10^5 MD steps), but a longer period of approximately 10^4 LJ units (or 10^6 MD steps) is required before the number of free molecules equilibrates. The time required to equilibrate the number of free molecules increases with increasing α, increasing roughly proportionately to $1/c_1$. (This follows from the fact that the the rate of insertion per micelle is given by a product of the insertion rate constant and c_1, and that the insertion rate constant for micelles of a specified aggregation number depends very little on α.) The resulting small decrease in micelle aggregation number also has less effect on other properties as α increases, however, simply because the average number of free molecules released from the micelle becomes very small for large values of α.

Throughout these simulations, we use the cluster identification algorithm to identify fission events. Immediately after we turn off the external potential that is used to pre-assemble a micelle, this algorithm identifies one large cluster that contains all of the copolymers. Somewhat later, the algorithm normally finds one large cluster and a few free molecules. Potential fission events are identified by determining the earliest time at which this algorithm finds two clusters with aggregation numbers that are both greater than some cutoff value a, for which we choose $a = 10$. For the appearance of a second large cluster to qualify as a fission event, we also require that almost all of the molecules in these two clusters be molecules that were part of the single large cluster just prior to this event.

Figure 7 shows a coarse histogram of the distribution of values for the ratio of the aggregation number of each daughter micelle produced by a fission event to the aggregation number of the parent micelle. The results shown here for each value of α are averaged over several values of the aggregation number n of the parent cluster. The fact that the distribution is clustered around a 50/50 split confirms that the fission events identified here usually produce two daughter clusters of approximately equal size.

We have observed that, under some conditions, a second micelle can appear within our simulation cell via step-wise association of free molecules, rather than via fission of the pre-assemble micelle. This was observed only at the lowest value of α considered here, $\alpha = 10$, for which stepwise association is more frequent, and only for systems with relatively small values of N. Observation of stepwise association becomes more likely with decreasing N at a fixed value of α because the increase in intrinsic fission lifetime with decreasing aggregation number leaves more time for stepwise association to preempt fission. Formation of a micelle by stepwise association is characterized by appearance a second cluster of size $n \geq n_{cut}$ in which the smaller such cluster initially has an aggregation number $n = a$, because it has grown by stepwise insertion from a cluster with $n < a$, and in which few if any of the molecules in this smaller cluster were recently members of the single larger cluster.

We did not attempt to estimate τ_n^{fis} under conditions for which any stepwise association events were observed. This requirement limited the lower end of the range of values of n over which we could obtain a reliable value for τ_n^{fis} at $\alpha = 10$, but had no effect on our analysis of results obtained with other values of α.

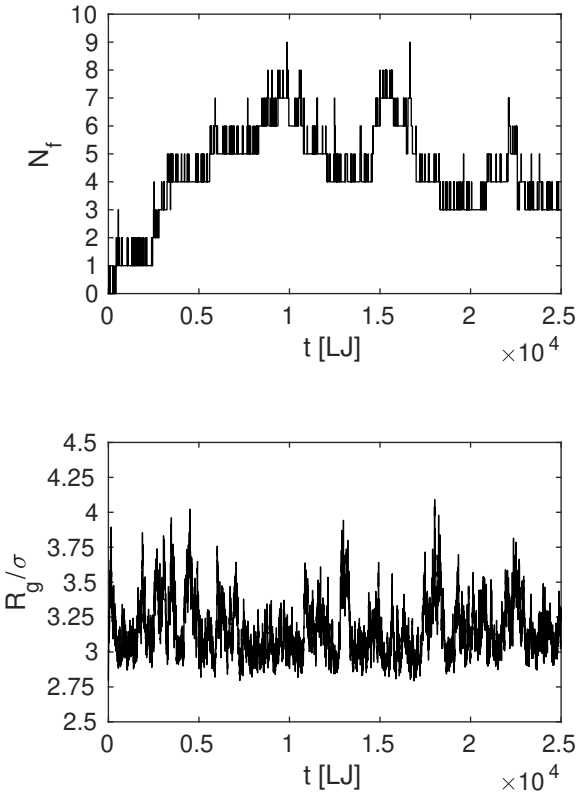

FIG. 6. These plots show the time dependence of the radius of gyration of the micelle core, denoted by R_g (lower plot) and the number N_f of free surfactant molecules (upper plot) as a function of time t after initiation of a fission simulation. Data shown here is for a system of $N = 140$ surfactant molecules and $\alpha = 14$, for which the average final aggregation number is $n \approx 136$. Time t is given in Lennard-Jones time units, where $t = 0$ corresponds to the time at which the potential that we use to a assemble a micelle is removed. For this system, the relaxation time for the radius of gyration is less than 10^3 LJ time units, while the relaxation time for the number of free surfactant molecules is approximately 10^4 LJ time units.

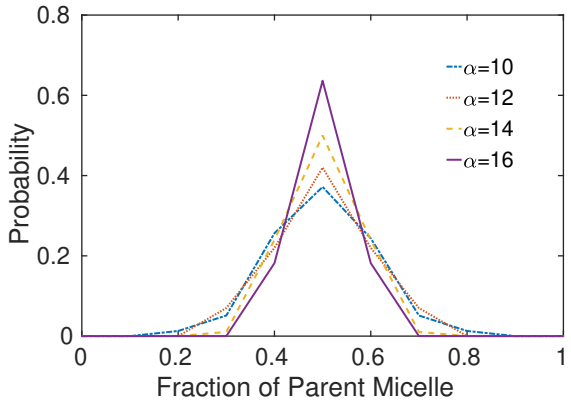

FIG. 7. Histogram of values of the ratio of aggregation number of each daughter produced by a fission event to the aggregation number of the parent micelle before fission. To obtain adequate statistics, the histogram is binned into ranges of value of width 0.1, so that, for example, the point at 0.4 represents the probability of finding a daughter for which this ratio lies between 0.35 and 0.45.

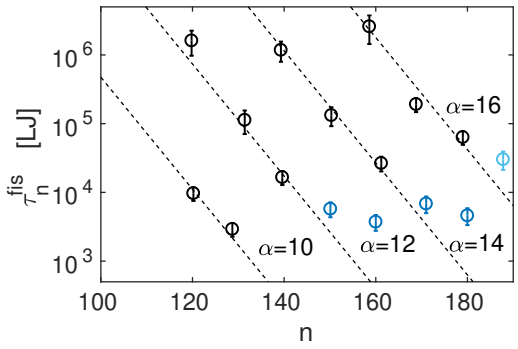

FIG. 8. Estimated values of the intrinsic fission lifetime τ_n^{fis} for micelles of differing size at $\alpha = 10$, 12, 14, and 16. Error bars show the root mean-squared statistical errors on the estimated value. Dashed lines show the predictions of the global linear fit to a function $\ln \tau_n^{fis}(\alpha) = A + B\alpha + Cm$ given in Eq. (8), plotted vs. n at these four values of α. Time is given in Lennard-Jones units, with 1 Lennard-Jones time τ_0 being equal to 200 MD steps. Symbols shown in black were used in the used to obtain Eq. (32), while lighter blue symbols obtained at higher values of n were excluded from the fit.

For each pair of values of α and N, we performed simulations of n independent systems for an equal time T after removal of the external potential used to assemble each micelle. The simulation time T used for each choice of α and N was chosen (based on information from preliminary simulations) so that roughly half of the micelles were expected to undergo fission during the course of the the simulation. When each such set of simulation were complete, we could identify a subset of systems in which fission occured during the simulation, for which we identify the time at which fission occurred.

If we had run these simulations long enough for all of the micelles to fission, the fission lifetime could have been estimated by simply taking the mean value of all measured fission times. A more sophisticated analysis is required to estimate a lifetime from results of simulations that are run for a finite time T comparable to the instrinsic lifetime, as done here. We have estimated τ_n^{fis} and the root-mean-squared statistical error of the estimate using a maximum likelihood estimator [54], as discussed in appendix D.

B. Results

Fig. 8 shows the estimated values of τ_n^{fis} plotted vs. aggregation number n for all four values of α considered here. Values of n shown in the absicca of this plot are mean values of the micelle aggregation number just prior to fission, as measured by a cluster identification algorithm, averaged over systems with the same values of α and N that undergo fission during the simulation. Error bars in this plot show the estimated root-mean-squared statistical error for τ_{fis}. Because of the relatively small sample size, the statistical error is substantial (typically 20 - 30% of τ_n^{fis}), but not large enough to obscure underlying trends.

Results for τ_n^{fis} show a clear systematic dependence upon both n and α. At each value of α, results for $\ln \tau_n^{fis}$ decrease approximately linearly with increasing n near the lower end of the range shown here, but crossover to a slower decrease at higher values of n. The behavior at high values of n appears consistent with saturation to a nearly constant value. Within the range of linear dependence of $\ln \tau_n^{fis}$ on n, the slope appears to be similar for different values of α. Within this regime, our results are fit rather well by an assumed linear dependence $\ln \tau_n^{fis}$ upon both n and α, of the form

$$\ln \tau_n^{fis} = A + B\alpha + Cn \quad , \tag{32}$$

with coefficients $A = 10.855$, $B = 2.0984$, and $C = -0.1877$. Dotted lines in Fig. 8 show lines predicted by this fit at constant values of $\alpha = 10$, 12, 14 and 16. This fit was obtained by fitting only the data points shown in black in 8, while excluding the points at higher values of n that are shown in blue.

Our ability to obtain meaningful results for τ_n^{fis} for very large values of n is limited, in part, by the requirement that this fission lifetime must be greater than the time required for an artificially pre-assembled micelle to reach a metastable local equilibrium state after the potential that we use to assemble the micelle is turned off. If this condition were not satisfied, then the measured fission lifetime could be sensitive to details of the procedure used to produce a pre-assembled initial state. For all of the data shown in Fig. 8, the observed value of τ_n^{fis} remains greater than the time required for apparent equilibration of fluctuations of the radius of gyration of the micelle core, which we use as an indicator of structural

relaxation of a micelle of fixed aggregation number. For some large values of n, the value of τ_n^{fis} measured here does, however, become comparable to the time required for a pre-assembled micelle to expel a few molecules and thereby reach an equilibrium average aggregation number.

For some of the largest micelles studied here, the micelle can thus undergo fission while the aggregation number is still (on average) slowly decreasing slightly by random expulsion of unimers. There are, however, two reasons to believe that this does not significantly effect our conclusions regarding the dependence of τ_n^{fis} on n. The first reason is the fact that the aggregation number shown as the absicca in Fig. 8 is actually the average aggregation number of micelles that fission, measured immediately prior to fission. We assume that the value of n just prior to fission is what controls the stability of the micelle with respect to fission, even in a simulation in which the average aggregation number is still slowly decreasing over the period when most fission events occur. The second reason is that, for the largest values of α considered here, the average number of molecules that would be expelled if the micelle did not undergo fission is simply too small to matter. The number of free molecules that would coexist in the simulation cell with a known total number of copolymers is analyzed in Appendix A in I. For $\alpha = 16$, we know that only 1-2 free molecules would coexist with the micelle at any value of n considered here. A change in n by 1-2 molecules would be too small to significantly change the expected value of τ_n^{fis}. For both of these reasons, we thus believe that the apparent tendency of τ_n^{fis} to saturate at large values of n is a real physical effect, rather than an artifact arising from slow changes in aggregation number. The evidence for this is particularly clear for $\alpha = 16$, for which the change in n is too small to matter.

Some level of understanding of how micelle structure varies with aggregation number can be obtained by reexamining Fig. 6 of I. This figure shows the root-mean-square core radii along principal directions of the gyration tensor plotted vs. n for systems with $\alpha = 12$ and $\alpha = 16$. A comparison of Fig. 6 of I and Fig. 8 of this work shows that at both of these values of α, the smallest value of n for which we have reported a fission time is slightly above the range in which Fig. 6 of I shows evidence of the start of a transition from a spherical shape to a dumbbell or slightly elongated rod. Over the range of values of n in which we were able to directly measure fission rates, the micelles thus appear to have cores are typically ellipsoidal or "pill" shaped prior to fission.

We show in Sec. XI that the overall fission rate in an equilibrated solution is dominated at each value of α by fission of micelles with aggregation numbers greater than the most probable value n_e but somewhat less than the smallest values for which we have been able to directly measured τ_n^{fis}. In what follows, we thus use Eq. (32) primarily to extrapolate our measurements of τ_n^{fis} to values of n that are less than those for which measurements were performed. The nature of the dependence of τ_n^{fis} on n at very large values of n, where this dependence is not adequately described by Eq. (32), is thus irrelevant to our analysis of overall fission rates in equilibrium.

X. SMOLUCHOWSKI MODEL

As a baseline for comparison to our measured fission rates, we now consider fusion and fission rates predicted by the Smoluchowski model discussed in subsection IV B, which assumes that micelle fusion is diffusion controlled.

Calculation of fusion rate constants for the Smoluchowski model is straightforward. The rate constant $k_{n,n'}^+$ for fusion between micellar clusters of aggregation numbers n and n' is given by Eqs. (16) and (17). The effective hard-core radius R_n used in Eq. (17) is taken to be the idealized core radius for a cluster of aggregation number n, defined as discussed previously. The effective diffusivity for each micelle has been computed by using a fit to the dependence of hydrodynamic radius on n shown in Fig. 2, while assuming negligible dependence of R_g on α at fixed n.

In order to allow comparison to our MD results, we focus on predictions of this model for fission rates. The intrinsic fission rate $k_n^{fis} = 1/\tau_n^{fis}$ measured in our simulations is the overall rate constant for fission of a parent cluster of aggregation number n into daughters of unspecified sizes. This is given by the sum of the rate constants for fission into all possible pairs of daughters. Using the detailed balance condition, $k_{n,n'}^- c_{n+n'}^* = k_{n,n'}^+ c_n^* c_{n'}^*$, k_n^{fis} can be expressed in terms of fusion rate constants as a sum

$$k_n^{fis} = \frac{1}{c_n^*} \sum_{n' \le n/2} k_{n',n-n'}^+ c_{n'}^* c_{n-n'}^* \quad . \tag{33}$$

By using the values of c_n^* obtained in paper I, we can thus compute predictions of this model for the fission lifetime $\tau_n^{fis} = \frac{1}{k_n^{fis}}$.

Fig. 9 shows the resulting predictions of values of τ_n^{fis} as a function of aggregation number n. For comparison, this figure also shows the results for τ_n^{fis} obtained from MD simulations, which are also shown in Fig. 8. Dashed lines in Fig. 9 simply show predictions of the Smoluchowki model multiplied by factors of 10, 100, and 1000, which create a constant vertical offset on this semi-logarithmic plot. As expected, measured lifetimes of τ_n^{fis} are greater than those predicted by the Smoluchowski model within the range of values of n for which direct measurement was performed. At $\alpha = 10$, measurements of τ_n^{fis} were limited to rather large values of n, complicating a comparison to predictions of the Smoluchowski model. We thus focus primarily on higher values of α. For the remaining values of $\alpha = 12$, 14, and 16, the value of τ_n^{fis} at the lowest value of n for which this quantity has been measured is approximately 10^3 greater than the value predicted by the Smoluchowski model.

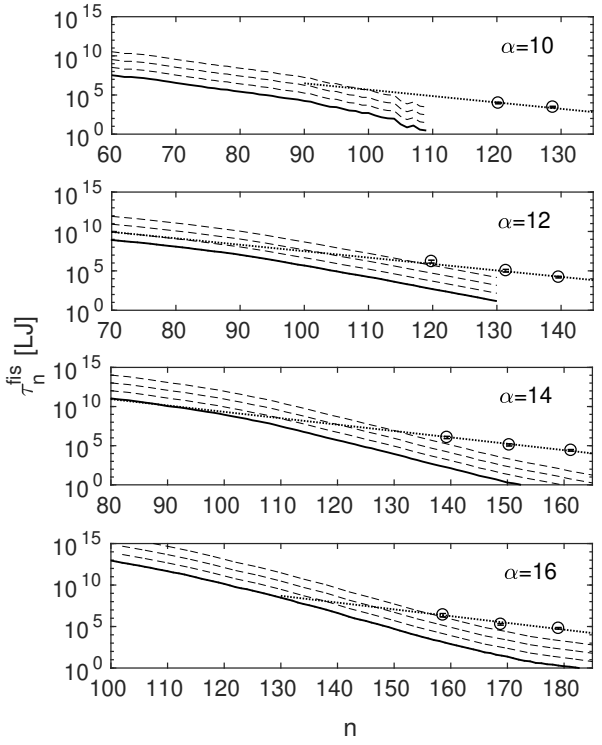

FIG. 9. Comparison of the measured values and predictions of the Smoluchowski theory for the fission lifetime τ_n^{fis}, plotted vs. aggregation number n. Solid black curves are predictions of the Smoluchowski theory. Dashed lines show predictions of the Smoluchowski theory multiplied by factors of $F = 10$, 100, and 1000. Open circles are values measured in MD simulations. Dotted straight lines are the fit to these measurements given by Eq. (32).

The key approximation underlying the Smoluchowski model is, of course, the neglect of any barrier to fusion. If there were instead a barrier to fusion of magnitude ΔG_n^{fus}, we would expect both fusion rates and corresponding fission rates to be decreased relative to that predicted by the Smoluchowski by an Arhenius factor $\exp(-\Delta G_n^{fus}/k_BT)$. For purposes of discussion, it is convenient for us to define an effective barrier ΔG_n^{fus} to fusion reactions that create an aggregate of aggregation number n by defining

$$e^{\Delta G_n^{fus}/k_BT} = \frac{\tau_n^{fis}}{\tau_n^{fis,S}} \tag{34}$$

where $\tau_n^{fis,S}$ denotes the intrinsic fission lifetime predicted by the Smoluchowski model, and τ_n^{fis} is the true fission lifetime. For reactions involving fission of relatively small micelles, we assume that this barrier is primarily due to the free energy required to deform the coronas of two colliding micelles in order to bring the micelle cores into intimate contact. Correspondingly, we picture the transition state for fusion as a state in which the approximately spherical cores of two micelles are nearly in contact but are connected by a thin throat of B-rich material. This picture suggests that the corresponding barrier should increase monotonically with increasing n, due to the larger free energy required to force together larger micelles in which the corona regions contain more molecules that become somewhat more strongly stretched with increasing n.

In the data shown in Fig. 9, the predictions of the Smoluchowski model for $\ln \tau_n^{fis}$ tend to decrease with increasing n more rapidly than the values measured in MD simulations. The effective barrier defined in Eq. (34) thus does appear to increase with increasing n. One consequence of this difference in slope in a plot of $\ln \tau_n^{fis}$ vs. n is that, for $\alpha = 16$, a simple linear extrapolation of the dependence of measured values of $\ln \tau_n^{fis}$ on n to lower values (the dotted line) would clearly intersect the predictions of the Smoluchowski model. Use of Eq. (32) to extrapolate to very small values of n would thus violate the lower bound provided by the Smoluchowski model. In order for the true fission lifetime τ_n^{fis} to be consistent with both our MD results and this lower bound, while also allowing for the existence of some barrier to fusion at all values of n, it seems clear that a plot of $\ln \tau_n^{fis}$ vs. n must curve upwards slightly at values of n below the range of n over which τ_n^{fis} has been measured. This behavior would naturally yield values of τ_n^{fis} that always exceed the greater of the value obtained from the Smoluchowski theory and the value obtained from the linear extrapolation given in Eq. (32), i.e., that satisfy

$$\tau_n^{fis} > \max(\tau_n^{fis,S}, \tau_n^{fis,L}) \tag{35}$$

where $\tau_n^{fis,S}$ denotes the prediction of the Smoluchowski model and $\tau_n^{fis,L}$ denotes the prediction of Eq. (32). We propose that this provides a tighter, and more physically reasonable lower bound on the fission lifetime than that provided by Smoluchowski model alone, which yields fission lifetimes that are known to be much too low at large values of n.

In order to examine the possible effects of the existence of a modest barrier to fusion for small micelles, we have also considered predictions of a family of models in which τ_n^{fis} is approximated as a function

$$\tau_n^{fis} = \max(F\tau_n^{fis,S}, \tau_n^{fis,L}) \tag{36}$$

where F is a constant factor. In this approximation, $F \equiv \exp(\Delta G^{fus}/k_BT)$ is a factor that has been introduced to take into account the effects of a barrier $\Delta G^{\dagger}$ that, for simplicity, been taken to be independent of n over the relevant range of values of n. Setting $F = 1$ in this approximation yields the lower bound given in Eq. (35). Values of $F\tau_n^{fis,S}$ for $F = 10$, 100, and 1000 are shown by dotted lines in Fig. 9. In order for this approximation to remain consistent with all measured values of τ_n^{fis}, the factor of F used for $\alpha = 14$ and F must be approximately 10^3 or less, corresponding to an effective barrier of $\Delta G^{fus} = \ln(10^3)k_BT = 6.9k_BT$ or less. On

physical grounds, we find it implausible that the deformation of the corona's required to bring the cores of two micelles into contact could not produce a free energy barrier of a least a few k_BT, making it hard to justify a value of $F < 10$. The comparison of MD results at large values of n with predictions of the Smoluchowski model thus yields a relatively narrow range (in a logarithmic sense) of plausible values of the factor of F or (equivalently) the effective barrier in this approximation.

XI. EQUILIBRIUM FISSION LIFETIME

We now consider the rate at which micelles undergo fission in equilibrium. Let r_{fis} denote the rate of fission events of proper micelles in an equilibrated solution, per unit volume and per unit time. This quantity can be expressed as a sum

$$r_{fis} = \sum_{n=a}^{\infty} c_n^* k_n^{fis} \quad , \tag{37}$$

where $k_n^{fis} = 1/\tau_n^{fis}$ is the intrinsic fission rate for micelles of aggregation number n. Here, a is a lower cutoff that we introduce to exclude fission of small submicellar aggregates. The corresponding equilibrium rate of fission per micelle, denoted here by k_f is given by the ratio

$$k_f = r_{fis}/c_{\rm mic} \tag{38}$$

where

$$c_{\rm mic} = \sum_{n=a}^{\infty} c_n^* \tag{39}$$

is the total equilibrium number concentration of micelles of size $n \geq a$. Let τ_f denote the equilibrium fission lifetime, which is defined to be the inverse

$$\tau_f = 1/k_f \tag{40}$$

of this rate of fission per micelle.

A. Distribution of Fission Reactants

To identify which micelles undergo fission most frequently, it is useful to also consider the probability that a random fission event involved fission of a micelle of aggregation number n. This probability, denote by $P_{fis}(n)$, is proportional to the equilibrium rate of fission of n-mers, and is thus given to within a constant by the product

$$P_{fis}(n) \propto k_n^{\rm fis} c_n^* \quad . \tag{41}$$

Because the intrinsic fission rate k_n^{fis} increases with increasing aggregation number, while c_n^* decreases with increasing n for $n > n_{\rm e}$, we expect $P_{fis}(n)$ to reach a maximum at a value of n somewhat greater than n_{eq}.

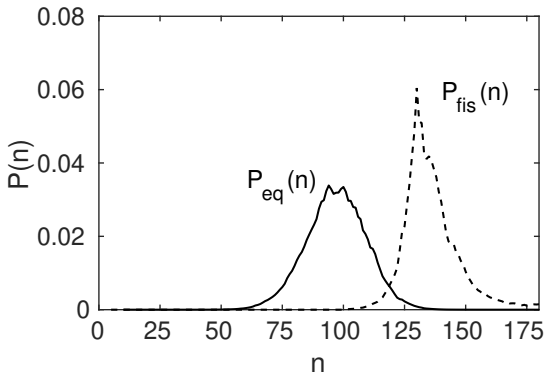

FIG. 10. Comparison of the equilibrium micelle distribution $P_{eq}(n)$ with the distribution $P_{fis}(n)$ of fission reactants for a system with $\alpha = 16$ and $\Delta\mu = \Delta\mu_{\rm c}$, plotted vs. micelle aggregation number n. For $P_{fis}(n)$, n refers to the aggregation of the parent (reactant) micelles. Both distributions have been normalized so that the sum over integer values of n greater than a cutoff is equal to unity. The equilibrium distribution $P_{eq}(n)$ is proportional to the equilibrium number concentration $P_{eq}(n) \propto c_n^*$, while $P_{fis}(n)$ is given by Eq. (41).

Computation of the equilibrium fission rate and lifetime is straightforward given estimates of both the equilibrium concentration c_n^* and the intrinsic fission rate k_n^{fis} as functions of n over the physically relevant range. Values for equilibrium concentrations have been accurately determined for this model over a wide range of values of n. Values for intrinsic fission rate constants have, however, been measured only over a more limited range of rather large values of n. To obtain a simple estimate of equilibrium fission rate, we have thus taken the empirical formula given in Eq. (32) to apply at arbitrary values of n, thus using Eq. (32) to extrapolate our measurements of k_n^{fis} to values of n less than than the lower limit of the range over which direct measurements were performed.

Figure 10 shows the predictions obtained for $P_{fis}(n)$ by this approximation alongside corresponding results for the equilibrium micelle size distribution $P_{eq}(n)$ for systems with $\alpha = 16$. The predicted value for $P_{fis}(n)$ shows a maximum at a value of $n \simeq 128$ roughly 30 % greater than the value $n_{\rm e} \simeq 97$ at which $P_{eq}(n)$ is maximum. Fission of a micelle of this size into two daughters of equal size would lead to two micelles of size $n \simeq 64$ that are substantially smaller than the most probable size. After fission, the aggregation numbers of these fission products would begin to fluctuate via much more frequent stepwise insertion and expulsion events. Because these fission products in this example would have aggregation numbers much greater than the critical aggregation number for dissociation but greater than $n_{\rm e}$, they would be unlikely to dissociate, and will instead tend to revert to the most probably value $n_{\rm e}$ via stepwise insertion.

These results suggest the following scenario for a typical fission event: A micelle chosen at random from the equilibrium distribution fluctuates in size as a result of

comparatively frequent insertion and expulsion events. Fission is a much more rare event that usually occurs during a rare fluctuation when n is signficantly greater than n, and creates two micelles of aggregation numbers significantly less than n. In systems in which stepwise processes are much more frequent than fusion or fission events, these fission products are very likely to to grow to aggregation numbers near n_e by stepwise insertion before having time to undergo fusion or any other more rare process. Further quantitative justification for this scenario is provided in appendix C, in which we which compare time scales for different possible processes involving products of a fission reaction.

Because fusion and fission must obey detailed balance, the most common fusion events must involve fusion of aggregates with the same sizes as the most common products of fission events. Because fission is known to usually yield two products of similar aggregation number, the most common fusion events for the example of a system with $\alpha = 16$ must involve fusion of micelles with aggregation numbers equal to roughly half the value at which $P_{fis}(n)$ is maximum, i.e., fusion of micelles with $n \simeq 64$. One may see from inspection of the equilibrium distribution $P_{\rm eq}(n)$ shown in Fig. 10 that such small micelles are relatively rare. This implies that both fusion and fission usually involve rare clusters that appear in the tails of the equilibrium distribution, with fission typically occuring for clusters with $n > n_e$ and fusion typically occuring for clusters with $n < n_e$.

B. Comparison of Different Estimates

The above analysis yields a prediction for $P_{fis}(n)$ for systems with $\alpha = 16$ with a maximum at a value that is signficantly below the smallest value of $n \simeq 160$ at which we actually were able to measure a fission rate. Similar analyses at other values of α yield similar results: The value of n for which events are predicted to be most frequent is greater than the most probable size n_e but is always somewhat less than the lower limit of the range over which we were able to measure $k_n^{\rm fis}$. The accuracy of our estimate of the equilibrium lifetime τ_f thus depends critically upon the accuracy of whatever approximation we use to estimate τ_n^{fis} outside the range of values of n in which we measured $k_n^{\rm fis}$.

In what follows, we discuss estimates of τ_f that are based on several different approximations for the dependence of τ_n^{fis} on n.

(a) *Smoluchowski Model*: We have computed an estimate of τ_f by using the predictions of the Smoluchoski model for τ_n^{fis} at all n.

(b) *Equation (32)*: We have obtained a simple estimate by using Eq. (32) to approximate τ_n^{fis} at all n, thus assuming a strictly linear dependence of $\ln \tau_n^{fis}$ on n.

(c) *Equation (36)* with varying values of F: Several related estimates of τ_f have computed by using Eq. (36) for τ_n^{fis} with values of F =1, 100, and 1000.

(d) *Upper Bound on* τ_f: We have constructed an upper bound on τ_f by applying Eq. (32) over the range of values of large values of n within which this approximation is reliable, and simply ignoring the possibility of fission of micelles for which n falls outside this range.

Comments about these estimates are given below.

The use of the Smoluchowski model (estimate a) provides a lower bound on the value of τ_{fis} that can be constructed without reference to the results of our MD simulations of fission rates for large micelles. Because the model predicts unphysically rapid fission for large micelles, however, it yields an estimate of τ_n^{fis} that is much less than any estimate that takes into account the results of our MD simulations for fission rates.

The estimate obtained by using Eq. (36) (estimate c) with $F = 1$ represents the bound given in Eq. (36). We believe that this extimate represents the lowest value that τ_f could plausibly have in light of the results of our MD simulations and the bound on τ_n^{fis} provided by Smoluchowski theory. Estimates computed with Eq. (36) with values of $F > 1$ provide information about how the presence of a modest barrier to fusion would effect computed fission rates.

To construct an upper bound for τ_f (estimate d), we used Eq. (32) for τ_n^{fis} for all values of n for which this equation yields $\tau_n^{fis} < 5 \times 10^6$ LJ units and simply set $k_n^{\rm fis} = 0$ for all smaller values of n. This cutoff on the maximum allowed value of τ_n^{fis} is slightly greater than the greatest value that we were able to measure for $\alpha =$ 12, 14, or 16, and corresponds to the upper edge of the plot shown in Fig. 8. For the case $\alpha = 16$, this bound causes us to neglect of fission for all parent micelles with $n < 158$. By inspection of Fig. 10, one can see one can see that this cutoff ignores the overwhelming majority of fission events, and must thus produce an estimated fission rate much lower than the true rate. This upper bound was computed for all $\alpha \geq 12$ but not for $\alpha = 10$, because of the limited range of values of n over which we could reliably estimate $\tau_n^{\rm fis}$ for $\alpha = 10$.

Fig. 8 shows a comparison of estimates for τ_f obtained by all of the methods described above. Several conclusions emerge from an inspection of this graph.

Predictions of τ_f obtained using the Smoluchoski model (open circles) are several orders of magnitude lower than those obtained by any other method. This is a result of the unrealistically short fission lifetimes predicted by this model for large values of n, which are dramatically faster than the results of our MD simulations in the same range of n. This estimate can thus be discounted as unrealistically fast.

The estimate obtained using Eq. (32) (+ symbols, estimate b) is very similar, but slightly less than the estimated obtained using Eq. (36) and $F = 1$. These two

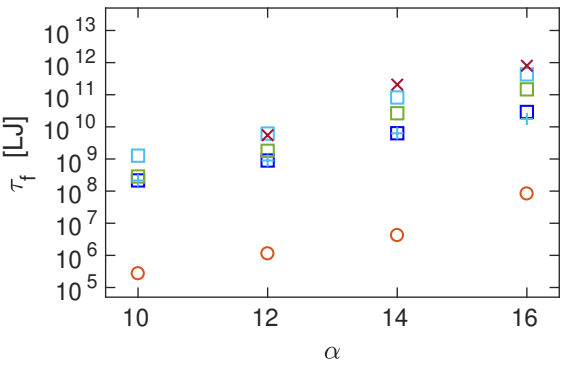

FIG. 11. Comparison of several different estimates of the equilibrium fission lifetime τ_f. Open circles are calculated using the Smoluchowski model (estimate a). Plus (+) symbols represent estimate obtained by using Eq. (32) for τ_n^{fis} for all n (estimate b). Open squares represent estimates obtained by using Eq. (36) with different values of F =1, 100, 1000, from lowest to highest (estimate c). Cross (×) symbols represent the upper bound by allowing for fission of only very large micelles for which the behavior of τ_n^{fis} is known from MD simulations (estimate d).

estimates are similar because both estimates predict that most fission events involve micelles with n in a range of values in which Eq. (32) yields a larger estimate of τ_n^{fis} than the Smoluchowski theory. The estimate obtained using Eq. (36) is, however, necessarily greater than or equal to that obtained from Eq. (36) because Eq. (36) yields an estimate of τ_n^{fis} that is greater than obtained from Eq. (32) for all values of n.

Upon comparing estimates obtained using Eq. (36) with different values of F, we see that the range of values predicted for τ_f is much narrower than the range of values of F considered, again because many of the fission events occur in a range of values of n in which the value given by Eq. (36) is equal to that given by Eq. (32). The value obtained using $F = 1000$ also comes rather close to the upper bound obtained by ignoring the contribution of fission involving micelles for which n lies below the range in which it has been measured. This is because the assumption of such a large value for F shifts the distribution $P_{fis}(n)$ to higher values of n.

The true value of τ_f for this model cannot be determined exactly from the available data, but almost certainly lies somewhere between the estimate obtained by using Eq. (32) with $F = 1$ and that obtained using $F = 10^3$. We suspect that the most accurate estimate may be that provided by using Eq. (32) using $F = 100$. More important, however, is the observation that the comparison of these estimates seems to constrain the plausible range of values to a range of approximately one order of magnitude or less at each value of α, with a value $\tau_f \sim 10^{11}$ for the highest value of $\alpha = 16$. It is also worth noting that this range of possible values for the equilibrium fission lifetime τ_f seems to increase much less rapidly with increasing α than our estimate of the the equilibrium dissociation lifetime, increasing only about 2-3 orders of magnitude as α increases from 10 to 16, rather than the 6 order of magnitude change predicted for τ_d. A direct comparison of our estimates of τ_d and τ_f is deferred to the final section of this paper.

XII. DISCUSSION AND CONCLUSIONS

This work is a quantitative study of the rates of several different types of infrequent dynamical processes in a simple simulation model of a micellar solution of AB diblock copolymer surfactant in a solvent of A homopolymers. Specifically, we focus here on quantifying rates for "stepwise" insertion and expulsion of individual molecules, and rates of processes that can create and destroy entire micelles.

A. Insertion and Expulsion

Our analysis of insertion and expulsion rates focused on a comparison of the rate constant for insertion to the predictions of a diffusion limited insertion model. We chose to focus on predictions for insertion because the rate constant for insertion is simpler to interpret than the rate constant for expulsion. The rate constant for insertion is sensitive to the barrier posed by the corona (if any), but not to the large free energy required to remove the core block of the copolymer from the micelle core, which is the dominant factor determining the value of the expulsion rate. The question of whether the corona poses a significant barrier can thus be determined by comparing the insertion rate constant to a simple model of diffusion-controlled insertion. We find that, for the model studied here, insertion is completely diffusion limited, and that the corona surrounding each micelle thus does not present a significant barrier to insertion. This fact was demonstrated most directly by showing that the rate constant for insertion into a micelle is essentially indistinguishable from the corresponding rate constant for insertion into a homopolymer droplet with a radius equal to the radius of the micelle core.

The fact that the corona poses almost no barrier to insertion in this model may be a result of the particular choice of molecules and parameters used here, and need not be true more generally about block copolymer micelles. The barrier to insertion posed by the corona of an AB diblock is related to the stretching free energy of the corona chains, since the free energy required to drag the corona block of a free copolymer into the micelle corona is similar to the stretching free energy of chains that are already part of the micelle. The corona in the system studied here remains rather weakly stretched both as the result of our use of a polymeric solvent, rather than a small molecule solvent, and the use of relatively modest values of χN. The corona is more likely to present a

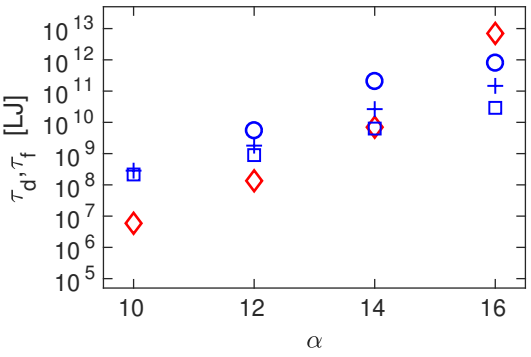

FIG. 12. Comparison of the dissociation lifetime τ_d to several different estimates of equilibrium fission lifetime τ_f, plotted vs. α. Red open diamonds show computed values of τ_d. Blue symbols show three different estimates of τ_f. Open circles are the upper bound on τ_f that we obtained by ignoring fission of micelles with lifetimes too long to be accurately measured by MD simulation. Plus signs are the estimate obtained by using Eq. (36) with $F = 100$, which is our best estimate of τ_f. Open squares are obtained using Eq. (36) with $F = 1$, which is the lowest estimate that is consistent with our MD results.

barrier to insertion in systems of long, comparatively insoluble copolymers dissolved in a small molecule solvent.

B. Micelle Creation and Destruction

The analysis of micelle creation and destruction processes given in Secs. VIII-XI focused on the computation or estimation of rates of the competing mechanisms of stepwise association and dissociation vs. fission and fusion. Figure 12 shows a comparison of predictions for the equilibrium dissociation lifetime τ_d (red diamonds) to three different estimates of the equilibrium fission lifetime τ_f. The three estimates of τ_{fis} include a strict upper bound (estimate d, open circles), a lower bound on the range of estimates consistent with our MD results (estimate c with $F = 1$, squares), and our proposed best estimate (estimate c with $F = 100$, shown by + signs).

The predicted dissociation lifetime τ_d can be seen to increase with increasing α (or decreasing surfactant solubility) much more rapidly than any of our three estimates of the equilibrium fission lifetime τ_f. As a result, there appears to be crossover within the range of parameters studied here from a regime of comparatively high copolymer solubility (low α) in which micelles are created by association and dissociation to a regime of lower solubility (high α) in which the number of micelles changes primarily by fission and fusion. The fact that $\tau_f < \tau_d$ at the highest value of $\alpha = 16$ is shown definitively by the fact that the computed value of τ_d (which is known quite accurately), is approximately 10 times greater than the upper bound on τ_f (open circles) that we obtained by ignoring the vast majority of fission events and only counting those involving unusually large, unstable micelles with an intrinsic lifetime short enough for us to measure. Conversely, it is clear that for $\alpha = 12$, τ_f is more than an order of magnitude less than the lowest of these three estimates of τ_f.

The results indicate that, for simple non-ionic surfactants of the type described by this model, stepwise association and dissociation control the slow process for relatively soluble surfactants, but that fission and fusion can dominate for less soluble surfactants. This conclusion is consistent with the conclusions of a number of authors [17, 21, 22, 32, 33] who have previously argued on experimental grounds that the slow process may occur by fission and fusion in this type of system (i.e., in systems of sparingly soluble non-ionic surfactants). The most important reason for the crossover from a stepwise mechanism to a fission-fusion mechanism is the rapid increase in the barrier ΔW_d to dissociation with increasing α or decreasing solubility, which causes the dissociation lifetime to increase more rapidly with decreasing solubility than the fission lifetime.

The accuracy of the estimates of fission lifetime given here is limited by our use of brute force MD simulations to estimate fission lifetime, which allowed us to estimate intrinsic lifetimes only for rather large, unstable lifetimes. We have worked around this limitation by combining these simulation results with predictions of the Smoluchowski theory to construct upper and lower bounds on τ_f, and found that these bounds were sufficient to establish the existence of a change in the mechanism of micelle birth and death with increasing α. It would be useful for further work along these lines to apply more sophisticated methods of estimating rates of rare processes in order to allow precise estimates of fission and fusion rate constants to be obtained over a wider range of values of aggregation number.

ACKNOWLEDGMENTS

This work was supported primarily by NSF grant DMR-1310436, with partial support from the NP and MP programs of the University of Minnesota Industrial Partnership for Interfacial and Materials Engineering (PRIME) center. We acknowledge the Minnesota Supercomputing Institute (MSI) at the University of Minnesota for providing computational resources for the work reported here. We are also grateful to Charles Geyer of the University of Minnesota School of Statistics for his help with statistical analysis of the fission lifetimes.

Appendix A: Finite-Size Effects on Diffusivity

When performing explicit solvent simulations via molecular dynamics with periodic boundary conditions complications can arise due to long range hydrodynamic interaction between a diffusing object and its periodic

images. In a cubic box of dimensions $L \times L \times L$, the relative magnitude of this effect depends upon the ratio of the hydrodynamic radius R_h to the box dimension L. For $L \gg R_g$, this effect has been shown to yield a correction to the apparent given by to a first order in $1/L$ by [50, 52]

$$D(L) = D - \frac{\xi k_B T}{6\pi\eta L} \tag{A1}$$

where D denotes the diffusivity in an infinite system, $D(L)$ is the measured apparent diffusivity in a periodic cubic cell with sides of length L, η is the fluid viscosity, and $\xi = 2.8372$ is a constant that was obtained by analyzing the equivalent hydrodynamics problem [52].

The hydrodynamic radius R_h is related to the diffusivity D in an infinite domain by the Stoke-Einstein relation $D = k_B T/(6\pi\eta R_h)$. The finite size correction given in Eq. (A1) yields a small fractional correction to D only only if $L \gg R_h$. In the simulations presented here, we found that this condition was satisfied in simulations of free molecules, for which $R_h/L \simeq 0.02$ for a typical value of $L \simeq 25\sigma$. In many of our simulations of micelles, however, the ratio R_h/L was found to be large enough to cause an appreciable error.

To test whether the dependence of our results on L can be described by this analytic theory, we have compared theoretical predictions to measurements of the apparent diffusivity $D(L)$ for micelles of aggregation numbers 20, 40, 60 and 80 in boxes with side lengths of length $L = 20$, 30, 40 and 80σ. This data was compared to a prediction for the dependence of $D(L)$ on $1/L$ that is accurate to order $\mathcal{O}(L^{-2})$, for which the theory predicts

$$D(L) = \frac{k_B T}{6\pi\eta}\left[\frac{1}{R_h} - \frac{1}{L}\left(\xi - \frac{4\pi R_h^2}{3L^2}\right)\right] \quad . \tag{A2}$$

Figure 13 shows a plot of the resulting measurements of $D(L)$ plotted vs. $1/L$, along with a fit of the results for each aggregation number to Eq. (A2), in which the true value of R_h for each micelle aggregation number has been treated as a fitting parameter. The quality of the fit confirms the validity of Eq. (A2).

After confirming that Eq. (A2) accurately described the data shown in Figure 13, values of R_h for other choices of n and α were found by measuring the apparent diffusivity $D(L)$ for each micelle aggregation number in a single box with $L = 25.2\sigma$ and then solving Eq. (A2) for R_h.

Appendix B: Computing Dissociation Lifetime

In this section, we discuss the computation of the micelle dissociation lifetime τ_d, computed within the context of a model of purely stepwise kinetics. We consider a system with a unimer concentration c_1 and micelle free energy W_n at that value of c_1 with a local maximum at

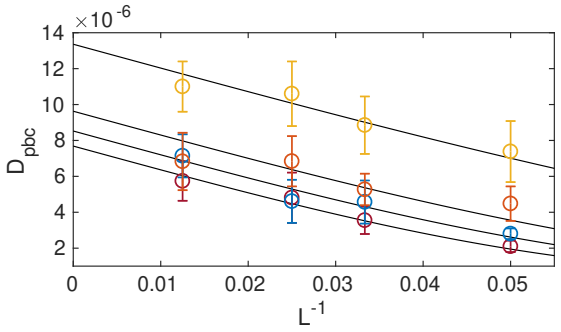

FIG. 13. Fit of the apparent diffusivity as a function of inverse box length for micelles of different aggregation numbers. From top to bottom the data is for aggregation numbers 20, 40, 60 and 80. Data was collected from 25 independent trajectories. Error bars are for one standard deviation from the mean.

n_t and a local miniminum n_e, for which the difference $\Delta W_d = W_a - W_{n_e}$ acts as a barrier to dissociation.

To compute τ_d, we analyze the thought experiment proposed in Sec. VIII. We imagine that at some time $t = 0$, we label all "proper" micelles of aggregation number n great than some cutoff size b in an equilibrated solution, for some choice of cutoff $b \in [n_t, n_e]$. Let $c_n(t)$ denote the population of micelles that had aggregation number $n > b$ at $t = 0$ and that have aggregation number n at time t, and that have survived over the interval $[0, t]$ without undergoing dissociation into unimers. A micelle will be assumed to be doomed to dissociation, and thus removed from the population of surviving micelles, if its aggregation number ever shrinks to a lower cutoff value a, for some choice of $a \in [1, n_t]$. The resulting estimate of τ_d will be almost independent of our exact choice of values for the cutoffs a and b, as long as these values are chosen appropriately. The value of b should be far enough below n_e so that, in equilibrium, almost all micelles have $n > b$. The value of a must be far enough below n_t so that a cluster of size a would be very unlikely to grow into a proper micelle before undergoing dissociation.

The concentration $c_n(t)$ described above is assumed to obey the master equation for the stepwise model, as given in Eqs. (11). The assumption that clusters of size $n \leq a$ are doomed to dissocation is implemented by imposing an absorbing boundary condition requiring that $c_n(t) = 0$ for $n = a$. The initial condition described above requires that $c_n(t = 0) = c_n^*$ for $n > a$ and $c_n(t = 0) = 0$ for $n \leq a$ at $t = 0$.

The evolution of the surviving subpopulation $c_n(t)$ is described by a system of ordinary differential equations (ODEs) that are linear in the concentration of clusters of sizes $n > a$. The resulting equations involve terms of the form $k_n^+ c_n c_1$ that arise from insertion reactions. The existence of such terms would yield a set of nonlinear equations if we allowed c_1 to vary with time, and thus treated $c_1(t)$ as one of our dynamical variables. We would, for example, have to allow for a time-dependent unimer con-

centration in order compute the "slow" time measured in experiments that probe the response of a micellar solution to a small step perturbation (e.g., a temperature jump). In the thought experiment that we consider here, however, we consider the evolution of a labelled subpopulation of clusters within a system that remains in equilibrium, and in which c_1 thus remains strictly constant.

Let $c_m(t)$ denote the total concentration of surviving micelles of aggregation number $n > b$ at time t, as given by the sum

$$c_m(t) = \sum_{n=b+1}^{\infty} c_n(t) \quad . \tag{B1}$$

This quantity to decays with time as a result of the flux in aggregation-number space to the absorbing boundary at $n = a$. At long times, $c(t)$ can be shown to exhibit an exponential decay

$$c(t) \propto e^{-t/\tau_d} \quad , \tag{B2}$$

in which τ_d is the desired dissociation lifetime. In the remainder of this section, we present two complementary methods of computing τ_d.

1. Eigenvalue Analysis

The conceptually simplest method of computing τ_d is based on the use of an eigenvector expansion to describe the relaxation of $c_n(t)$ for $n > a$. The set of linear ODEs that describe the time evolution of this model can be expressed as a matrix equation of the general form

$$\frac{d\mathbf{c}(t)}{dt} = -\mathbf{A}\mathbf{c}(t) \quad . \tag{B3}$$

Here, $\mathbf{c}(t)$ is a column vector whose elements are values of the concentration $c_n(t)$ for $n > a$, and in which $\mathbf{A}$ is a constant matrix. The matrix $\mathbf{A}$ can be shown to be a positive semidefinite tridiagonal matrix with constant elements whose values depend upon the constant c_1 and the rate constants k_n^+ and k_n^-.

The solution of Eq. B3 for the column vector $\mathbf{c}(t)$ can be expanded in terms of the eigenvectors of the matrix $\mathbf{A}$. Let $\mathbf{v}_\alpha$ for any $\alpha \geq 1$ denote an eigenvector of $\mathbf{A}$ that satisfies

$$\mathbf{A}\mathbf{v}_\alpha = \Gamma_\alpha \mathbf{v}_\alpha \quad , \tag{B4}$$

where Γ_α is an associated eigenvalue, and $\alpha = 1, 2, 3, \ldots$ is an index for independent eigenvectors. The solution of Eq. (B3) can be expanded in these eigenvectors as a sum

$$\mathbf{c}(t) = \sum_{\alpha \geq 1} d_\alpha \mathbf{v}_\alpha e^{-\Gamma_\alpha t} \quad . \tag{B5}$$

in which values of the coefficients $d_1, d_2, \ldots$ are chosen so as to satisfy the initial conditions requiring that $c_n(t = 0) = c_n^*$, and in which the eigenvalues $\Gamma_1, \Gamma_2, \ldots$ are all positive.

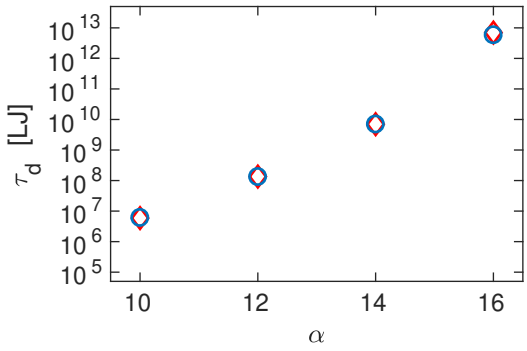

FIG. 14. Comparison of the stepwise dissolution of micelles at equilibrium by both the eigenvalue and Becker-Döring methods. Dark red diamonds correspond to the calculation obtained by numerical analysis of eigenvalues, while light blue circles symbols correspond to results of the Becker-Döring analysis.

Using the eigenvector expansion of $\mathbf{c}(t)$ to compute the sum $c_m(t)$ defined in Eq. (B1) would yield a sum of exponentially decaying contributions, in which each term arises from one of the eigenvectors, and the decay rate of each term is given by corresponding eigenvalue Γ_α. At very long times, the terminal decay is given by the lowest eigenvalue, which we denote by Γ_1, giving $c_m(t) \propto e^{-\Gamma_1 t}$. We thus identify the dissociation time τ_d as the inverse

$$\tau_d = 1/\Gamma_1 \tag{B6}$$

where Γ_1 is the lowest eigenvalue of $\mathbf{A}$.

The dissociation lifetime τ_d has been computed for the simulation model of interest at each of the four values of α used in our simulations, for systems with $c_1 = c_c$ or (equivalently) $c = 2c_c$. Very similar estimates of τ_d have been obtained by using the eigenvalue method described above and the Becker-Döring method described in the next subsection. Results obtained by both methods are shown in Figure 14.

2. Becker-Döring Analysis

The eigenvalue analysis discussed above provides a straightforward numerical algorithm for computing τ_d, by computing eigenvalues of a large matrix. It involves very few limiting assumptions, but also provides very little physical insight into what determines τ_d. In systems with a large barrier to dissociation, more insight can be gained by following method analogous to one that was originally introduced by Becker and Döring to describe homogeneous stepwise nucleation from a supersaturated vapor[30].

We again consider the decay of the population $c_n(t)$ of micelles that have survived over a time interval $[0, t]$.

The Becker-Döring analysis of dissociation is based on an assumption of quasi-steady decay during the late states of decay. In this approximation, we assume that the current $J_n(t)$ is independent of n over a range of values near n_t where $c_n(t)$ is very small. It is convenient to define a ratio

$$y_n(t) = c_n(t)/c_n^* \quad . \tag{B7}$$

where c_n^* is the equilibrium concentration of n-mers. The current $J_n(t)$ can be expressed in terms of $y_n(t)$ as a difference

$$J_n = -k_n^- c_{n+1}^* (y_{n+1} - y_n) \quad . \tag{B8}$$

We assume that $J_n(t)$ is equal to an n-independent value J for all n in some range $[a, b]$ that includes the transition state value n_t. By solving for $y_{n+1} - y_n$ for each $n \in [a, b]$, adding these differences of neighboring values, and setting $y_a(t) = 0$ to impose an absorbing boundary, we obtain

$$y_{b+1}(t) = -J(t)R \quad , \tag{B9}$$

in which

$$R = \sum_{n=a}^{b} \frac{1}{k_n^- c_{n+1}^*} \tag{B10}$$

is an effective steady-state "resistance".

To compute a dissociation rate, we assume in addition that the concentrations of proper micelles, of sizes $n > b$, retain a partial equilibrium distribution during the late stages of decay. A partial equilibrium distribution is one in which the ratio of concentrations $c_n/c_{n'}$ for micelles of different aggregation numbers $n, n' > b$ always has the value $c_n^*/c_{n'}^*$ that would be obtained in complete equilibrium. Such a state is characterized by a dimensionless concentration $y_n(t)$ that is independent of n, giving

$$y_n(t) = Y(t) \tag{B11}$$

for all $n > b$, where $Y(t)$ is a function that decays with time but that is independent of n. Setting $y_{b+1} = Y(t)$ in Eq. (B9) yields a flux

$$J(t) = -Y(t)/R \quad . \tag{B12}$$

The same approximation yields a total concentration $c_m(t)$ of proper micelles given by

$$c_m(t) = Y(t) c_m^* \quad , \tag{B13}$$

in which

$$c_m^* \equiv \sum_{n=b+1}^{\infty} c_n^* \tag{B14}$$

is the equilibrium concentration of micelles with $n > b$ at the specified unimer concentration.

The dissociation time can be determined by setting

$$\frac{dc_m(t)}{dt} = J(t) \quad , \tag{B15}$$

while using Eq. (B12) for $J(t)$ and (B13) for $c_m(t)$. Solving for $Y(t)$ then yields an exponential decay, $Y(t) \propto e^{-t/\tau_d}$, with a decay time

$$\tau_d = R c_m^* \quad . \tag{B16}$$

Eq. (26) in the main text is obtained by evaluating this product and making convenient choices for limits on the resulting summations.

The Becker-Döring analysis of τ_d is strictly valid only for systems with a large barrier to dissociation, $\Delta W_d \gg k_B T$. In this limit, the sum in Eq. (B14) for c_m^* is dominated by values of $n \simeq n_e$, while the sum in Eq. (B10) for R is instead dominated by values of $n \simeq n_t$. In the same limit, the values of R and c_m^* are both rather insensitive to the values chosen for the cutoff b used in the above analysis. In the expression given in Eq. (26), for simplicity, we have taken the sum that defines R to extend over all $n \leq n_e$ and taken the sum that defines $c_m^*(t)$ over all $n \geq n_t$.

Predictions for τ_d obtained using Eq. (26) are compared to those obtained by the eigenvalue method in Figure 14. For the model considered here, these methods yield results that agree within a few percent at all values of α. We chose to discuss only the Becker-Döring method in the body of the paper because it is more standard and provides a clear basis for discussing trends.

Appendix C: Fate of Fission Fragments

In subsection XI.A, we describe a scenario for a typical fission event. Fission was shown to usually involve a reactant with an aggregation number significantly greater than n_e (but less than $2n_e$) and to product products with aggregation numbers less than n_e but greater than the critical value n_t for stepwise dissociation. Here, we show that the product of such a fission event is very likely to grow to an aggregation number near n via stepwise processes before any competing process (e.g., dissociation or fusion) could occur. To do so, we compare estimates of characteristic time scales for several processes that can occur to products of a fission reaction.

Let P_n denote the normalized distribution of aggregation numbers of micelles that are created by fission, at the rates found in thermal equilibrium. This distribution is given to within a prefactor by a sum

$$P_n \propto \sum_{n'=1}^{\infty} k_{n,n'}^- c_{n+n'}^* \quad , \tag{C1}$$

with a prefactor chosen to satisfy the condition $\sum_n P_n = 1$. It is useful in this context to express $k_{n,n'}^-$ as a product

$$k_{n,n'}^- = k_{n+n'}^- P_{n,n'}^- \quad , \tag{C2}$$

in which k^-_{n+n} is the overall fission rate constant for clusters of aggregation number $n+n'$ and $P_{n,n'}$ is the probability that fission of such a cluster will produce fragments of specified sizes n and n'. Because the probability $P^-_{n,n}$ is largest for $n \simeq n'$, we expect P_n to be peaked about a most probable size approximately half the value of n for which the reaction rate $k^-_n c^*_n$ is maximum.

In what follows we consider the fate of a subpopulation of fission products that are produced at $t = 0$ with a distribution P_n, and estimate characteristic times for relaxation to the equilibrium distribution by stepwise processes, for stepwise dissociation, and for fusion processes. For concreteness, we focus in what follows on a system with $\alpha = 16$. In this case, fission is most frequent for reactants with $n \simeq 135$. We thus expect a distribution P_n peaked about a value $n \simeq 65$ that is intermediate between the most probable equilibrium value, $n_{\rm e} \simeq 100$, and the critical value for dissociation, $n_{\rm t} \simeq 20$.

We first consider the time for relaxation of the average aggregation number of such a subpopulation to the most probable value $n_{\rm e}$ by stepwise insertion and expulsion. To treat relaxation to equilibrium, it is useful to approximate the dependence of the micelle free energy W_n near its minimum by a harmonic function

$$W_n \approx W_{n_{\rm e}} + \frac{1}{2}\frac{k_B T}{\sigma^2}\left(n - n_{\rm e}\right)^2 + ... \qquad \text{(C3)}$$

in which σ is the standard deviation of n. If we adopt this approximate for n and approximate k^-_n by its value at $n = n_{\rm e}$, the stepwise model for diffusion of n becomes equivalent to a model of an overdamped Brownian harmonic oscillator with a diffusivity given by $k^-_{n_{\rm e}}$. The time scale τ for the relaxation of the average coordinate value of such a Brownian oscillator is given [55] by the ratio

$$\tau = \frac{\sigma^2}{k^-_{n_{\rm e}}} \quad , \qquad \text{(C4)}$$

where σ is the equilibrium standard deviation of n from $n_{\rm e}$. For $\alpha = 16$, we obtain $\sigma = 12.2$, $k^-_{n_{\rm e}} = 5.9 \times 10^{-4}$ inverse LJ time units, and $\tau \simeq 2.5 \times 10^6$ LJ time units for this process.

Stepwise dissociation is a more rare event that also occurs by stepwise processes. For a micelle with an initial aggregation number n in the range $[n_{\rm t}, n_{\rm e}]$, stepwise dissociation is always much less likely than relaxation to $n_{\rm e}$, simply because dissociation requires diffusion of n up a gradient in W_n to the maximum value at $n = n_{\rm t}$, rather than drift of n down the gradient to the minimum value of W_n at $n_{\rm e}$.

We next consider possibility that products of a fission reaction could undergo fusion with other micelles. The rate per unit time at which a micelle chosen at random from a population of size distribution P_n is given by a sum

$$\tau^{-1}_{fus} = \sum_{n,n'} P_n k^+_{n,n'} c^*_{n'} \quad . \qquad \text{(C5)}$$

The required fusion rate constant $k^+_{n,n'}$ is, of course related to $k^-_{n,n'}$ by the detailed balance condition $k^+_{n,n'} c^*_n c^*_{n'} = k^-_{n+n'} c^*_{n+n'}$. To estimate the fusion rate given in Eq. (C5), given knowledge of c^*_n for all n, it is thus sufficient to estimate $k^+_{n,n}$, which is also needed in Eq. (C1) for P_n. To estimate $k^+_{n,n}$ we have used an extrapolation of simulation results for the overall fission rate k^-_n and approximated $P_{n,n'}$ for fixed $n + n'$ by a Gaussian distribution that yields a distribution of values for products that is centered around half the reactant aggregation number with a standard deviation 6% of the reactant aggregation number. Using this estimate, we find a fusion lifetime $\tau_{fus} = 3.8 \times 10^8$ in Lennard-Jones units for a system with $\alpha = 16$. This is more than 100 times the estimated time for the average aggregation number to relax by stepwise insertion, implying that fusion is unlikely to occur befor relaxation of n stepwise insertion.

Appendix D: Statistical Analysis of Fission Data

We use a maximum likelihood estimator [54] to estimate the average fission lifetime $\tau_{fis}(M, \alpha)$ from our data for observed times of fission events. For each choice of a set of values of α and N, we perform n simulations of the same duration T, with $n = 20$. The results of the simulations yield a set of simulations in which fission occurred before the simulation was ended after a time T, and a set of simulations in which no fission was observed. If fission occurred in simulation number i, for $i \in [1, n]$ we define a variable y_i to be the time at which fission occurred. If fission did not occur in simulation number i, we set $y_i = T$, by convention.

We assume that survival to time y in each trial is controlled by an exponential probability density function

$$P(y;\tau) = \frac{1}{\tau} e^{-t/\tau} \qquad \text{(D1)}$$

for $y < T$, in which the parameter $\tau \equiv \tau_{fis}$ is the fission lifetime. There is also a probability $e^{-T/\tau}$ that fission will not occur before time T, corresponding to $y = T$. To derive an expression for the maximum likelihood estimator (MLE) for τ, we maximize the conditional probability of obtaining the observed sequence of values of $y_1, \ldots, y_n$ given a specified value of τ with respect to variations in the parameter τ. Because the n trials are statistically independent, the joint probability of obtaining a particular set of values $y_1, \ldots, y_n$, given a value for τ, is given by a product

$$P(y_1, \ldots, y_n; \tau) = P(y_1;\tau) P(y_2;\tau) \ldots P(y_n;\tau) \quad . \qquad \text{(D2)}$$

The maximumum likelihood estimator (MLE) for τ is obtained by setting the values of $y_1, \ldots, y_n$ to the observed values, with the understanding that values $y_i = T$ represents the case in which no fission occurs, and maximizing the joint probability $P(y_1, \ldots, y_n; \tau)$ with respect to the

unknown parameter τ. This can be done by maximizing the logarithm

$$\ln P(y_1, \ldots, y_n; \tau) = \sum_{i=1}^{n} \ln P(y_i; \tau) \quad , \tag{D3}$$

which is given explicitly by

$$\ln P(y_1, \ldots, y_n; \tau) = \sum_{i=1}^{n} B(y_i < T)(-y_i/\tau - \ln(\tau)) + \sum_{i=1}^{n} B(y_i = T)(-T/\tau) \quad , \tag{D4}$$

where $B(x)$ is a boolean-valued function that evaluates to 1 if its argument is a true statement and to 0 if its argument is false. The MLE is obtained by setting the derivative of this quantity with respect to τ equal to zero. A straightfoward calculation of the derivative yields the estimator

$$\tau = \frac{1}{m} \sum_{i=1}^{n} y_i \quad , \tag{D5}$$

in which n is the number of micelles that were observed to undergo fission before the end of the simulation (i.e., for which $y_i < T$). Here, a value $y_i = T$ is used in the sum for each simulations in which fission did not occur before the end of the simulation. The values shown in Fig. 8 of this supplementary material and Fig. 2 of the main manuscript are values of this estimator.

It is reassuring (for those of us who are not statisticians) to consider the behavior of this estimator in the limits of very long and very short simulations. In the limit of very long simulations, with $T \gg \tau$, we expect all micelles to undergo fission, giving $m = n$. In this case Eq. (D5) reduces to an expression for the average of the measured micelle lifetimes,

$$\lim_{T \gg \tau} \tau \simeq \frac{1}{n} \sum_{i=1}^{n} y_i \tag{D6}$$

with all $y_i < T$, as expected. In the opposite limit $T \ll \tau$, in which only a small fraction undergo fission, this estimator reduces to

$$\lim_{T \ll \tau} \tau \simeq Tn/m \quad , \tag{D7}$$

i.e., to T divided by the fraction that undergo fission in time T. This is consistent with the statement that, for $T \ll \tau$ and large n, the fraction that fission should approach T/τ.

The statistical error for a MLE of parameter τ can be estimated by computing the Fisher information, denoted here by I. The Fisher information for a measurement of n independent trials of a variable with a distribution $P(y; \tau)$ is given by the average

$$I = n \left\langle \frac{-\partial^2 \ln P(y; \tau)}{\partial \tau^2} \right\rangle \quad , \tag{D8}$$

in which

$$\langle \cdots \rangle = \int dy P(y; \tau) \cdots \tag{D9}$$

denotes an average computed with respect to the hypothesized probability distribution, using the estimated value of τ. The mean-squared statistical error σ^2 is given for $n \gg 1$ by the inverse Fisher information,

$$\sigma^2 \simeq 1/I \quad . \tag{D10}$$

We use this as our estimate of the RMS statistical error σ. For the model of $P(y; \tau)$ considered here, the required average is analytically tractable, and yields

$$\sigma = \tau / \langle m \rangle^{1/2} \tag{D11}$$

in which

$$\langle m \rangle = n[1 - \exp(-T/\tau)] \tag{D12}$$

is the expected mean value of the number m of simulations in which fission occurs before time T.

We are grateful to Prof. Charles Geyer of the University of Minnesota School of Statistics for suggesting the use of a maximum likelihood estimator, and providing us with the analysis outlined above. Prof. Geyer had assigned an equivalent problem as homework for a graduate class in statistics, and gave us the homework solution for reference.

[1] J. A. Mysona, A. V. McCormick, and D. C. Morse, Phys. Rev. E. (2019).
[2] G. Kresheck, E. Hamori, G. Davenport, and H. Scheraga, Journal of the American Chemical Society **88**, 246 (1966).
[3] K. Takeda and T. Yasunaga, Journal of Colloid and Interface Science **45**, 406 (1973).
[4] K. Takeda, T. Yasunaga, and S. Harada, Journal of Colloid and Interface Science **42**, 457 (1973).
[5] T. Inoue, R. Tashiro, Y. Shibuya, and R. Shimozawa, Journal of Colloid and Interface Science **73**, 105 (1980).
[6] S. Yiv, R. Zana, W. Ulbricht, and H. Hoffmann, Journal of Colloid and Interface Science **80**, 224 (1981).
[7] J. Lang and E. M. Eyring, Journal of Polymer Science **10**, 89 (1972).
[8] P. Mijnlieff and R. Dimarsch, Nature **208**, 889 (1965).

[9] P. Mukerjee and A. Ray, J. Phys. Chem **683**, 1947 (1963).
[10] B. C. Bennion and E. M. Eyring, Journal of Colloid and Interface Science **32**, 286 (1970).
[11] J. Rassing, P. J. Sams, and E. Wyn-Jones, Journal of the Chemical Society, Faraday Transactions 2: Molecular and Chemical Physics **2**, 1247 (1974).
[12] T. Yasunaga, S. Fuji, and M. Miura, Journal of Colloid and Interface Science **30**, 399 (1969).
[13] T. Telgmann and U. Kaatze, J. Phys. Chem. B **101**, 7758 (1997).
[14] E. A. G. Aniansson and S. Wall, Journal of Physical Chemistry **78**, 1024 (1974).
[15] E. A. G. Aniansson and S. Wall, Journal of Physical Chemistry **79**, 857 (1975).
[16] E. Aniansson, S. Wall, M. Almgren, H. Hoffmann, I. Kielmann, W. Ulbricht, R. Zana, J. Lang, and C. Tondre, Journal of Physical Chemistry **80**, 905 (1976).
[17] M. Teubner and M. Kahlweit, Advances in Colloid and Interface Science **13**, 1 (1980).
[18] T. Zinn, L. Willner, R. Lund, V. Pipich, and D. Richter, Soft Matter **8**, 623 (2012).
[19] S. Choi, T. Lodge, and F. Bates, Physical Review Letters **104**, 047802 (2010).
[20] J. Lu, F. S. Bates, and T. L. Lodge, ACS Macro Lett **2**, 451 (2013).
[21] M. Kahlweit, Journal of Colloid and Interface Science **90**, 92 (1982).
[22] I. Griffiths, C. Bain, C. Breward, D. Colegate, P. Howell, and S. Waters, Journal of Colloid and Interface Science **360**, 662 (2011).
[23] I. M. Griffiths, C. J. W. Breward, D. M. C. adn P. J. Dellar, P. D. Howell, and C. D. Bain, Soft Matter **9**, 853 (2013).
[24] I. Nyrkova and A. Semenov, Macromolecular Theory and Simulations **14**, 569 (2005).
[25] R. Thiagarajan and D. Morse, Journal of Physics: Condensed Matter **23**, 284109 (2011).
[26] F. Kuni, A. Rusanov, A. Grinin, and A. Shchekin, Colloid Journal **63**, 197 (2001).
[27] F. Kuni, A. Rusanov, A. Grinin, and A. Shchekin, Colloid Journal **63**, 723 (2001).
[28] F. M. Kuni, A. I. Rusanov, A. K. Shchekin, and A. P. Grinin, Russian Journal of Physical Chemistry **79**, 833 (2005).
[29] A. K. Shchekin, L. T. Adzhemyan, I. A. Babinstev, and N. A. Volkov, Colloid Journal **80**, 107 (2018).
[30] R. Becker and W. Doering, Annalen der Physik **416**, 719 (1935).
[31] C. U. Herrmann and M. Kahlweit, J. Phys. Chem. **84**, 1536 (1980).
[32] D. Colegate, *Structure-kinetics relationships in micellar solutions of nonionic surfactants*, Ph.D. thesis, Durham University (2009).
[33] I. Griffiths, C. Breward, D. Colegate, P. Dellar, P. Howell, and C. Bain, Soft Matter **9**, 853 (2013).
[34] L. Meli, J. M. Santiago, and T. P. Lodge, Macromolecules **43**, 2018 (2010).
[35] E. Dormidontova, Macromolecules **32**, 7630 (1999).
[36] A. K. Shchekin, A. I. Zakharov, and L. T. Adzhemyan, J. Chem. Phys. **143**, 124902 (2015).
[37] A. K. Shchekin, I. A. Babintstev, and L. T. Adzhemyan, J. Chem. Phys. **145**, 174105 (2016).
[38] A. Halperin and S. Alexander, Macromolecules **22**, 2403 (1989).
[39] M. Sammalkorpi, M. Karttunen, and M. Haataja, J. Phys. Chem. B **111**, 11722 (2007).
[40] Z. Li and E. Dormidontova, Macromolecules **43**, 3521 (2010).
[41] S. Marrink, D. Tieleman, and A. Mark, J. Phys. Chem. B **104**, 12165 (2000).
[42] A. Sangwai and R. Sureshkumar, Langmuir **27**, 6628 (2011).
[43] M. Sammalkorpi, M. Karttunen, and M. Haataja, J. Am. Chem. Soc. **130**, 17977 (2008).
[44] J. Gao, S. Li, X. Zhang, and W. Wang, Phys. Chem. Chem. Phys. **12**, 3219 (2010).
[45] M. Velinova, D. Sengupta, A. V. Tadjer, and S.-J. Marrink, Langmuir **27**, 14071 (2011).
[46] Z. Li and E. Dormidontova, Soft Matter **7**, 4179 (2011).
[47] A. Prhashanna, S. A. Khan, and S. B. Chen, Macromolecular Theory and Simulations **25**, 383 (2016).
[48] R. Pool and P. G. Bolhuis, J. Chem. Phys. **126**, 244703 (20057).
[49] G. J. Martyna, D. J. Tobias, and M. L. Klein, J. Chem. Phys. **101**, 4177 (1994).
[50] I.-C. Yeh and G. Hummer, J. Phys. Chem. B **108**, 15873 (2004).
[51] N. A. Volkov, M. V. Posysoev, and A. K. Shchekin, Colloid Journal **80**, 248 (2018).
[52] H. Hasimoto, Journal of Fluid Mechanics **5**, 317 (1959).
[53] T. Ghasimakbari, *Simulation Studies of Correlations, Dynamics and Phase Transitions in Diblock Copolymer Melts*, Ph.D. thesis, University of Minnesota (2018).
[54] G. Casella and R. L. Berger, *Statistical Inference, 2nd ed.* (Duxbury Thomson Learning, 2002).
[55] M. Doi and S. F. Edwards, *The Theory of Polymer Dynamics* (Oxford University Press, 1986).